Decomposition Products of Phosphine Under Pressure: PH_2 Stable and Superconducting?

Andrew Shamp, Tyson Terpstra, Tiange Bi, Zackary Falls, Patrick Avery, and Eva Zurek

Contents

1 XTALOPT Searches Details

The XTALOPT evolutionary algorithm (EA)[S1,S2] was used for the structure searches. In this algorithm a new offspring is procreated as soon as an individual has finished optimizing. The parents are chosen from a population-based pool instead of being selected from structures in previous generations. Tables S1-S6 provide the population size of every EA search we have carried out for various stoichiometries, numbers of formula units, and pressures of the PH_n, $n = 1 - 6$, phases. We generally stopped each run after recovering at least 5 duplicates of the lowest-enthalpy structure, whose identity did not change over at least 100 structures. A six-step structural-optimization scheme was used for all runs, and each step employed the geometry of the optimized structure from the previous step as the initial geometry. The first two steps only allowed the ions to relax, while the remaining steps allowed both the ions and the lattice parameters to relax during the optimization. The precision of the calculation was increased in each step.

Stoichiometry	Formula Units	Pressure (GPa)	Population
PH	1	100	299
	2		299
	2		104
	3		299
	4		299
	5		298
	6		298
PH	1	150	299
	2		316
	3		65
PH	2	200	245
	3		179

Table S1: Number of formula units, and the size of the population used in the evolutionary structure searches for PH at 100, 150, and 200 GPa. In some instances multiple runs for a given system (e.g. 2 formula units of PH at 100 GPa) were carried out.

Stoichiometry	Formula Units	Pressure (GPa)	Population
PH_2	1	100	169
	2		169
	2		1702
	3		169
	3		1585
	4		169
	5		169
	6		168
	2	150	563
	3		509
	2	200	746
	3		604

Table S2: Same as Table S1 but for PH_2.

Stoichiometry	Formula Units	Pressure (GPa)	Population
PH_3	1	100	197
	2		196
	2		191
	3		196
	3		177
	4		196
	5		196
	6		196
	3		362
	4		361
	2	150	924
	2		238
	3		926
	3		131
	2	200	887
	2		143
	3		886
	3		200

Table S3: Same as Table S1 but for PH_3.

Stoichiometry	Formula Units	Pressure (GPa)	Population
PH_4	1	100	197
	2		190
	3		202
	4		213
	5		213
	6		209
	1	150	88
	2		81
	2		53
	2		357
	3		83
	4		90
	5		87
	6		93
	2	200	227
	3		185

Table S4: Same as Table S1 but for PH_4.

Stoichiometry	Formula Units	Pressure (GPa)	Population
PH_5	1	100	162
	2		162
	3		162
	4		162
	5		162
	6		162
	2	150	984
	3		982
	2		106
	2	200	294
	3		82

Table S5: Same as Table S1 but for PH_5.

Stoichiometry	Formula Units	Pressure (GPa)	Population
PH_6	1	100	362
	2		363
	3		362
	4		361
	2	150	924
	3		926
	2	200	887
	3		886

Table S6: Same as Table S1 but for PH_6.

2 Convergence Tests for the Cut-off Energy Used in the Plane Wave Basis Set

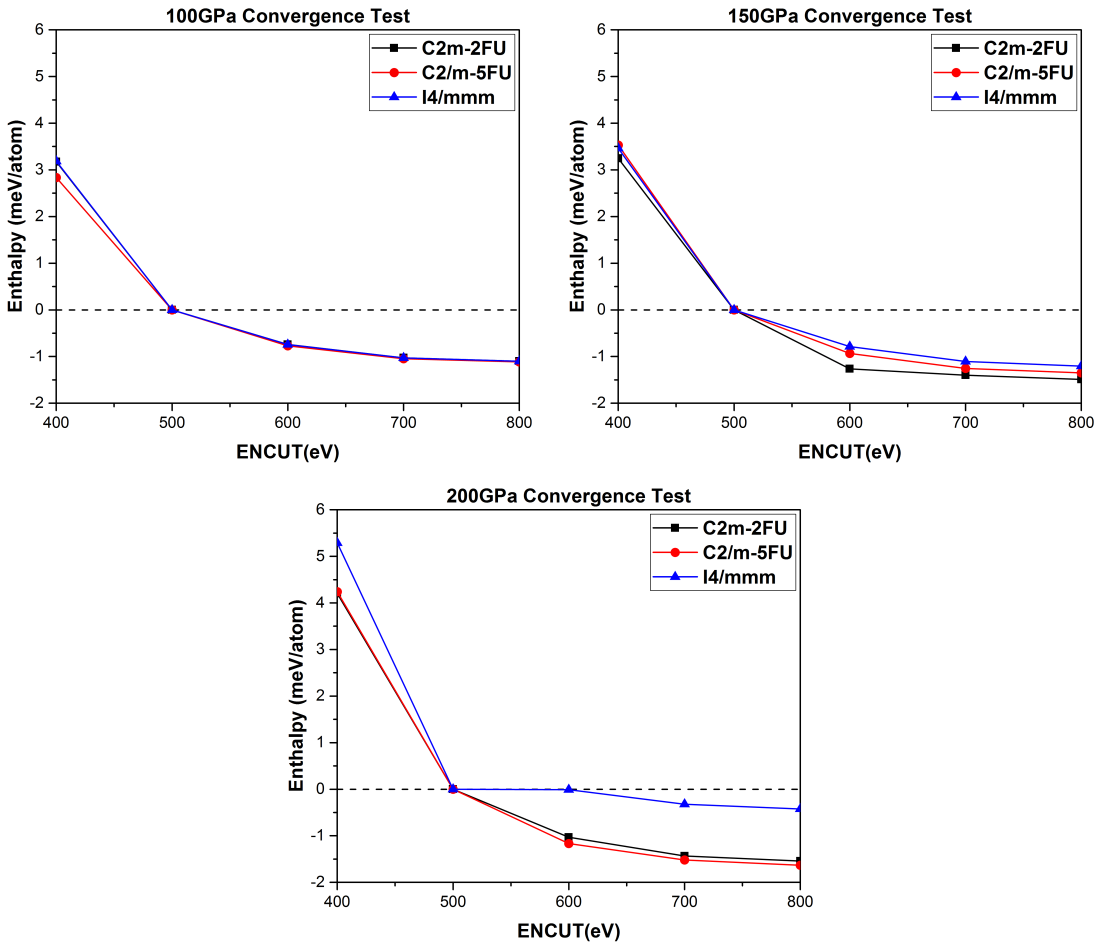

Figure S1: Relative enthalpies of the PH_2 phases at 100, 150 and 200 GPa as a function of the cut off energy used in the plane wave basis set (ENCUT). The relative enthalpies are given with respect to the enthalpy calculated using ENCUT of 500 eV. In the plot at 100 GPa, the data for 2FU-$C2/m$ (black line) is not seen because it overlaps with the data of 5FU-$C2/m$ and $I4/mmm$.

3 Structural Coordinates of High Pressure PH_2 Phases

3.1 5FU-*C2/m*

Pressure (GPa)	**100**
Enthalpy (E_h/F.U.)	**-0.01219**
a, b, c (Å)	6.029 2.151 11.156
α, β, γ (Θ)	90.00 104.84 90.00
H (4i)	0.52640 0.00000 0.81833
H (4i)	0.11053 0.00000 0.48231
H (4i)	-0.07083 0.00000 0.30677
H (4i)	0.41089 0.00000 0.42773
H (4i)	0.81058 0.00000 0.05645
P (2a)	0.00000 0.00000 0.00000
P (4i)	0.76516 0.00000 0.81688
P (4i)	0.17095 0.00000 0.36786
Pressure (GPa)	**150**
Enthalpy (E_h/F.U.)	**0.13952**
a, b, c (Å)	5.783 2.093 10.746
α, β, γ (Θ)	90.00 104.78 90.00
H (4i)	0.51445 0.00000 0.81722
H (4i)	0.11265 0.00000 0.48696
H (4i)	-0.07348 0.00000 0.30720
H (4i)	0.42339 0.00000 0.42967
H (4i)	0.80602 0.00000 0.05859
P (2a)	0.00000 0.00000 0.00000
P (4i)	0.75990 0.00000 0.81608
P (4i)	0.17524 0.00000 0.36921
Pressure (GPa)	**200**
Enthalpy (E_h/F.U.)	**0.27542**
a, b, c (Å)	5.592 2.051 10.439
α, β, γ (Θ)	90.00 104.62 90.00
H (4i)	0.50525 0.00000 0.81646
H (4i)	0.11526 0.00000 0.49141
H (4i)	-0.07596 0.00000 0.30760
H (4i)	0.43302 0.00000 0.43035
H (4i)	0.80188 0.00000 0.05983
P (2a)	0.00000 0.00000 0.00000
P (4i)	0.75566 0.00000 0.81547
P (4i)	0.17764 0.00000 0.37046

Table S7: Calculated structural coordinates and enthalpies of the 5FU-$C/2m$ PH_2 phase at 100, 150, and 200 GPa. The unit of enthalpies are given in Hartree per formula unit (E_h/F.U.)

3.2 2FU-*C2/m*

Pressure (GPa)	**100**
Enthalpy (E_h/F.U.)	**-0.01036**
a, b, c (Å)	3.056 3.046 3.352
α, β, γ (Θ)	90.00 117.12 90.00
H (4i)	0.25701 0.00000 0.51424
P (2b)	0.00000 0.50000 0.00000
Pressure (GPa)	**150**
Enthalpy (E_h/F.U.)	**0.13968**
a, b, c (Å)	2.989 2.979 3.160
α, β, γ (Θ)	90.00 118.21 90.00
H (4i)	0.75799 0.00000 0.51589
P (2b)	0.00000 0.50000 0.00000
Pressure (GPa)	**200**
Enthalpy (E_h/F.U.)	**0.27542**
a, b, c (Å)	5.152 2.961 2.960
α, β, γ (Θ)	90.00 90.23 90.00
H (4i)	0.27528 0.00000 0.58402
H (4i)	0.77498 0.00000 -0.08459
P (2b)	0.00000 0.50000 0.00000
P (2c)	0.00000 0.00000 0.50000

Table S8: Calculated structural coordinates of the 2FU-$C/2m$ PH_2 phase at 100, 150, and 200 GPa. The unit of enthalpies are given in Hartree per formula unit (E_h/F.U.)

3.3 *I4/mmm*

Pressure (GPa)	**100**
Enthalpy (E_h/F.U.)	**-0.01039**
a, b, c (Å)	2.158 2.158 5.965
α, β, γ (Θ)	90.00 90.00 90.00
H (4e)	0.00000 0.00000 0.25701
P (2b)	0.00000 0.00000 0.50000
Pressure (GPa)	**150**
Enthalpy (E_h/F.U.)	**0.13960**
a, b, c (Å)	2.109 2.109 5.574
α, β, γ (Θ)	90.00 90.00 90.00
H (4e)	0.00000 0.00000 0.24225
P (2b)	0.00000 0.00000 0.50000
Pressure (GPa)	**200**
Enthalpy (E_h/F.U.)	**0.27545**
a, b, c (Å)	2.077 2.077 5.574
α, β, γ (Θ)	90.00 90.00 90.00
H (4e)	0.00000 0.00000 0.22778
P (2b)	0.00000 0.00000 0.50000

Table S9: Calculated structural coordinates of the $I4/mmm$ PH_2 phase at 100, 150, and 200 GPa. The unit of enthalpies are given in Hartree per formula unit (E_h/F.U.)

4 Structural Coordinates of High Pressure PH_5 Phases

4.1 $P\bar{1}$

Pressure (GPa)	**100**
Enthalpy (E_h/F.U.)	**-0.14338**
a, b, c (Å)	4.701 3.375 3.146
α, β, γ (Θ)	117.75 88.72 107.40
H (2i)	0.37613 0.10476 0.43436
H (2i)	0.87159 0.19267 0.16999
H (2i)	-0.00499 0.69708 0.28701
H (2i)	0.44392 0.74303 -0.05968
H (2i)	0.74725 0.48159 0.63574
P (2i)	0.25554 0.24972 0.86866
Pressure (GPa)	**150**
Enthalpy (E_h/F.U.)	**0.08179**
a, b, c (Å)	4.505 3.246 3.011
α, β, γ (Θ)	62.57 88.91 106.58
H (2i)	0.37784 0.09698 0.32421
H (2i)	0.87377 0.20220 -0.03941
H (2i)	0.00380 0.69484 0.59893
H (2i)	0.44171 0.74613 0.18606
H (2i)	0.74513 0.47401 0.14856
P (2i)	0.25334 0.24682 0.61918
Pressure (GPa)	**200**
Enthalpy (E_h/F.U.)	**0.28175**
a, b, c (Å)	4.366 3.148 2.897
α, β, γ (Θ)	63.22 89.17 107.05
H (2i)	0.37944 0.08893 0.32019
H (2i)	0.87365 0.20441 -0.05620
H (2i)	0.00849 0.68846 0.61457
H (2i)	0.44016 0.74642 0.17580
H (2i)	0.74205 0.46463 0.14604
P (2i)	0.25149 0.24472 0.61831

Table S10: Calculated structural coordinates of the $P\bar{1}$ PH_5 phase at 100, 150, and 200 GPa. The unit of enthalpies are given in Hartree per formula unit (E_h/F.U.)

5 Structural Coordinates of High Pressure PH_3 Phases

5.1 *Pm*

Pressure (GPa)	**100**
Enthalpy (E_h/F.U.)	**-0.05229**
a, b, c (Å)	3.086 3.536 2.992
α, β, γ (Θ)	90.00 89.76 90.00
H (c)	0.16813 0.71436 0.79461
H (b)	0.61062 0.50000 0.75922
H (b)	0.25034 0.50000 0.27053
H (a)	0.31570 0.00000 0.22104
H (a)	0.60615 0.00000 0.83021
P (b)	0.70236 0.50000 0.22441
P (a)	-0.02794 0.00000 0.53824
Pressure (GPa)	**150**
Enthalpy (E_h/F.U.)	**0.12364**
a, b, c (Å)	2.980 3.388 2.868
α, β, γ (Θ)	90.00 89.34 90.00
H (c)	0.16416 0.71214 0.81535
H (b)	0.57831 0.50000 0.73009
H (b)	0.26472 0.50000 0.30082
H (a)	0.34111 0.00000 0.22286
H (a)	0.59030 0.00000 0.82660
P (b)	0.72017 0.50000 0.19272
P (a)	-0.02944 0.00000 0.52907
Pressure (GPa)	**200**
Enthalpy (E_h/F.U.)	**0.28190**
a, b, c (Å)	2.900 3.274 2.781
α, β, γ (Θ)	90.00 89.27 90.00
H (c)	0.16546 0.71348 0.83209
H (b)	0.55861 0.50000 0.70722
H (b)	0.26900 0.50000 0.32250
H (a)	0.35870 0.00000 0.22646
H (a)	0.57978 0.00000 0.82325
P (b)	0.72790 0.50000 0.16768
P (a)	-0.03143 0.00000 0.52158

Table S11: Calculated structural coordinates of the *Pm* PH_3 phase at 100, 150, and 200 GPa. The unit of enthalpies are given in Hartree per formula unit (E_h/F.U.)

5.2 *P1*

Pressure (GPa)	**100**
Enthalpy (E_h/F.U.)	**-0.05054**
a, b, c (Å)	4.923 3.294 2.145
α, β, γ (Θ)	109.00 77.43 95.48
H (a)	0.60847 -0.00128 0.38544
H (a)	0.25660 0.67488 0.39930
H (a)	0.42172 0.06309 0.01133
H (a)	0.83051 0.87151 0.71072
H (a)	0.03456 0.80209 0.07401
H (a)	0.44336 0.61049 0.77340
P (a)	0.14774 0.23333 0.23303
P (a)	0.71733 0.44026 0.55170
Pressure (GPa)	**150**
Enthalpy (E_h/F.U.)	**0.12257**
a, b, c (Å)	4.778 3.113 2.092
α, β, γ (Θ)	109.63 77.38 97.48
H (a)	0.59662 -0.02581 0.37934
H (a)	0.26846 0.69940 0.40539
H (a)	0.42643 0.06656 0.01159
H (a)	0.83226 0.89993 0.72412
H (a)	0.03282 0.77365 0.06061
H (a)	0.43865 0.60706 0.77315
P (a)	0.14755 0.23497 0.23380
P (a)	0.71752 0.43861 0.55093
Pressure (GPa)	**200**
Enthalpy (E_h/F.U.)	**0.27880**
a, b, c (Å)	4.650 2.988 2.058
α, β, γ (Θ)	69.89 77.23 90.13
H (a)	0.59416 -0.04988 0.41763
H (a)	0.27090 0.72349 0.69350
H (a)	0.43287 0.07005 -0.06260
H (a)	0.83771 -0.07951 0.81090
H (a)	0.02736 0.75312 0.30024
H (a)	0.43220 0.60351 0.17375
P (a)	0.14875 0.23747 -0.00276
P (a)	0.71633 0.43613 0.11391

Table S12: Calculated structural coordinates of the *P1* PH_3 phase at 100, 150, and 200 GPa. The unit of enthalpies are given in Hartree per formula unit (E_h/F.U.)

6 Relative Enthalpy and the Structural Coordinates of Reference Phosphorus and Hydrogen

6.1 Relative Enthalpy

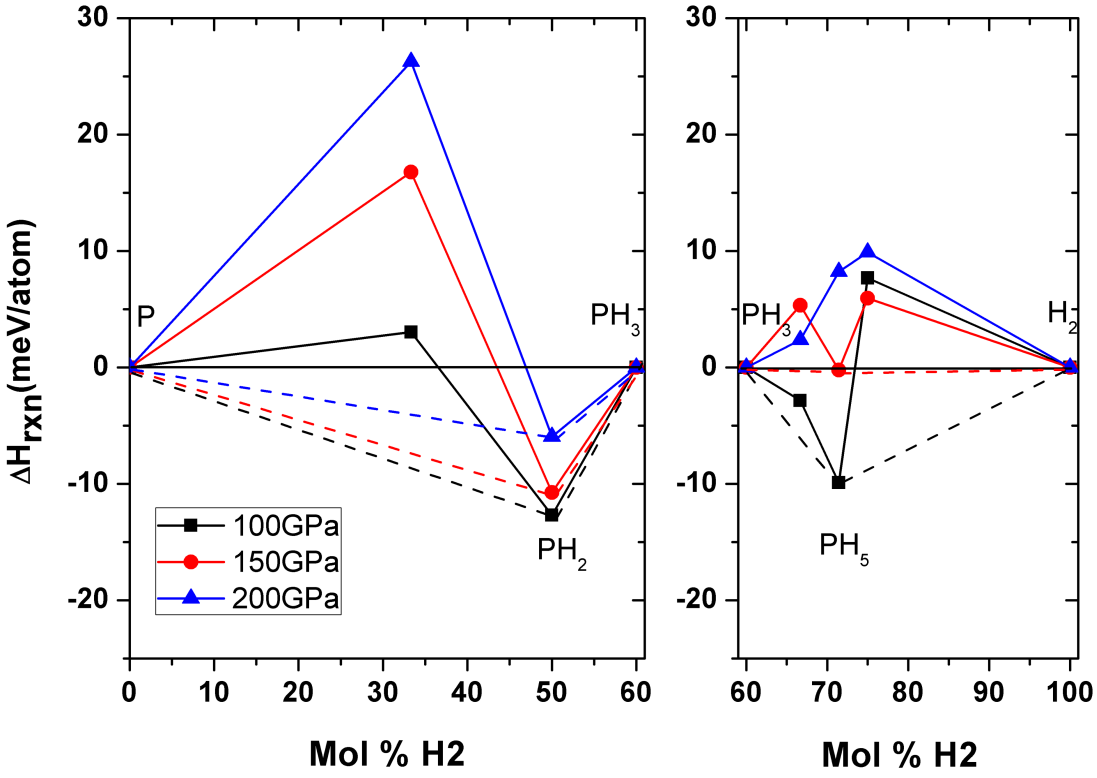

Figure S2: (a) ΔH_{rxn} for the reaction: (left) $PH_n \rightarrow (\frac{3-n}{3})P + (\frac{n}{3})PH_3$ (where $n = 0 - 3$) and (right) $PH_n \rightarrow (\frac{n-3}{2})H_2 + PH_3$ (where $n = 3 - 6$) at 100, 150, and 200 GPa. The convex hulls are given by the dashed lines.

6.2 Structural Coordinates and Enthalpies of Reference Phosphorus Phases

Pressure (GPa)	**100**
Enthalpy (E_h/atom)	**0.07255**
a, b, c (Å)	2.149 2.149 2.149
α, β, γ (Θ)	90.00 90.00 90.00
P (1b)	0.50000 0.50000 0.50000

Table S13: Structural coordinates of the simple cubic phosphorus phase at 100 GPa.[S3–S5] The unit of enthalpy is given in Hartree per atom (E_h/atom).

Pressure (GPa)	**150**
Enthalpy (E_h/atom)	**0.17703**
a, b, c (Å)	2.176 2.176 2.064
α, β, γ (Θ)	90.00 90.00 120.00
P (1b)	0.00000 0.00000 0.50000
Pressure (GPa)	**200**
Enthalpy (E_h/atom)	**0.27083**
a, b, c (Å)	2.124 2.124 2.023
α, β, γ (Θ)	90.00 90.00 120.00
P (1b)	0.00000 0.00000 0.50000

Table S14: Structural coordinates of the simple hexagonal phosphorus phase at 150 and 200 GPa.[S5] The unit of enthalpies are given in Hartree per atom (E_h/atom).

6.3 Structural Coordinates and Enthalpies of Reference Hydrogen Phases

Pressure (GPa)	**100**
Enthalpy (E_h/H_2)	**-0.08891**
a, b, c (Å)	3.769 3.769 3.001
α, β, γ (Θ)	90.00 90.00 120.00
H (6h)	0.39009 0.29172 0.25000
H (6h)	0.26600 0.06777 0.25000
H (4h)	0.33333 0.66667 0.12798

Table S15: Structural coordinates of the $P6_3/m$ hydrogen phase at 100 GPa.[S6] The unit of enthalpy is given in Hartree per H_2 (E_h/H_2).

Pressure (GPa)	**150**
Enthalpy (E_h/H_2)	**-0.04073**
a, b, c (Å)	3.094 5.385 5.540
α, β, γ (Θ)	90.00 90.00 90.00
H (4c)	0.35377 0.64736 0.12508
H (4c)	0.08456 0.28190 0.88497
H (4c)	0.08432 0.71293 0.35685
H (4c)	0.12605 0.50042 0.62633
H (4c)	0.64963 0.64672 0.12424
H (4c)	0.08702 -0.04590 0.84975
H (4c)	0.79602 0.49939 0.12555
H (4c)	0.07516 0.61896 0.88814
H (4c)	0.31196 0.68765 0.62803
H (4c)	0.07775 0.05114 0.40051
H (4c)	-0.08125 0.61796 0.36973
H (4c)	0.18569 0.81265 0.62081
Pressure (GPa)	**200**
Enthalpy (E_h/H_2)	**0.00114**
a, b, c (Å)	2.978 5.182 5.342
α, β, γ (Θ)	90.00 90.00 90.00
H (4c)	0.34739 0.65061 0.12523
H (4c)	0.08698 0.27624 0.88180
H (4c)	0.08654 0.71264 0.35908
H (4c)	0.13333 0.50054 0.62676
H (4c)	0.65089 0.65175 0.12430
H (4c)	0.09487 -0.04412 0.85388
H (4c)	0.80361 0.50123 0.12538
H (4c)	0.07207 0.61809 0.88797
H (4c)	0.31255 0.68505 0.62708
H (4c)	0.07746 0.05429 0.39657
H (4c)	-0.08743 0.61574 0.37068
H (4c)	0.17930 0.81751 0.62129

Table S16: Structural coordinates of the $b2/n$ hydrogen phase at 150 and 200 GPa.[S6] The unit of enthalpies are given in Hartree per H_2 (E_h/H_2).

7 2FU-*C2/m* and *I4/mmm* PH_2 Phases

7.1 Octahedral Canting Angles

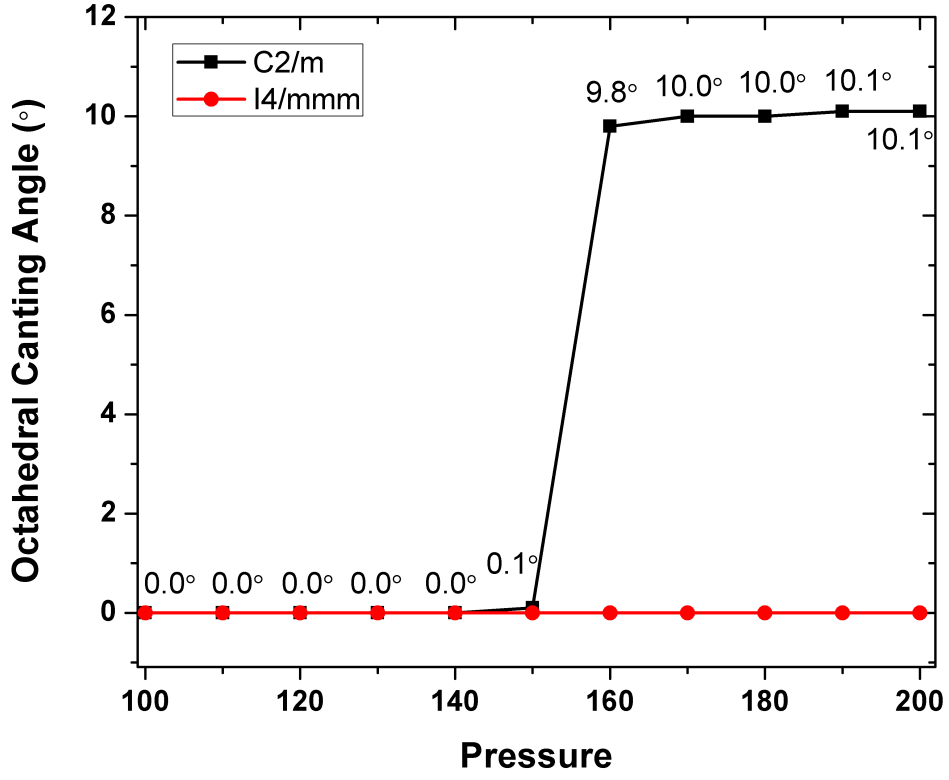

Figure S3: Comparion of calculated octahedral canting angles of 2FU-$C2/m$ and $I4/mmm$ phases in the pressure range between 100 and 200 GPa.

7.2 Internal Energy, PV Energy and Enthalpy

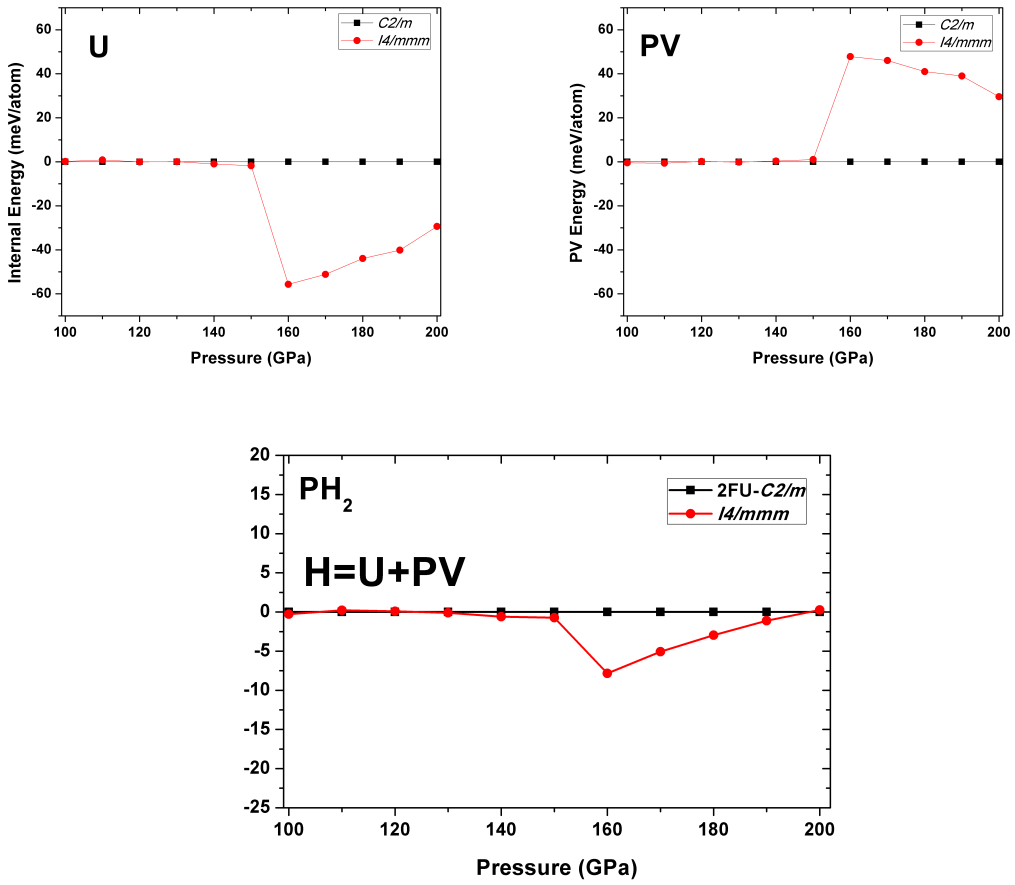

Figure S4: Comparison of calculated internal energy (U), PV (PV) and Enthalpy ($H = U + PV$) of 2FU-$C2/m$ and $I4/mmm$ phases in the pressure range between 100 and 200 GPa. Energies are given in meV/atom where the values for the $C2/m$ phase have been set to zero.

7.3 Relative Volume

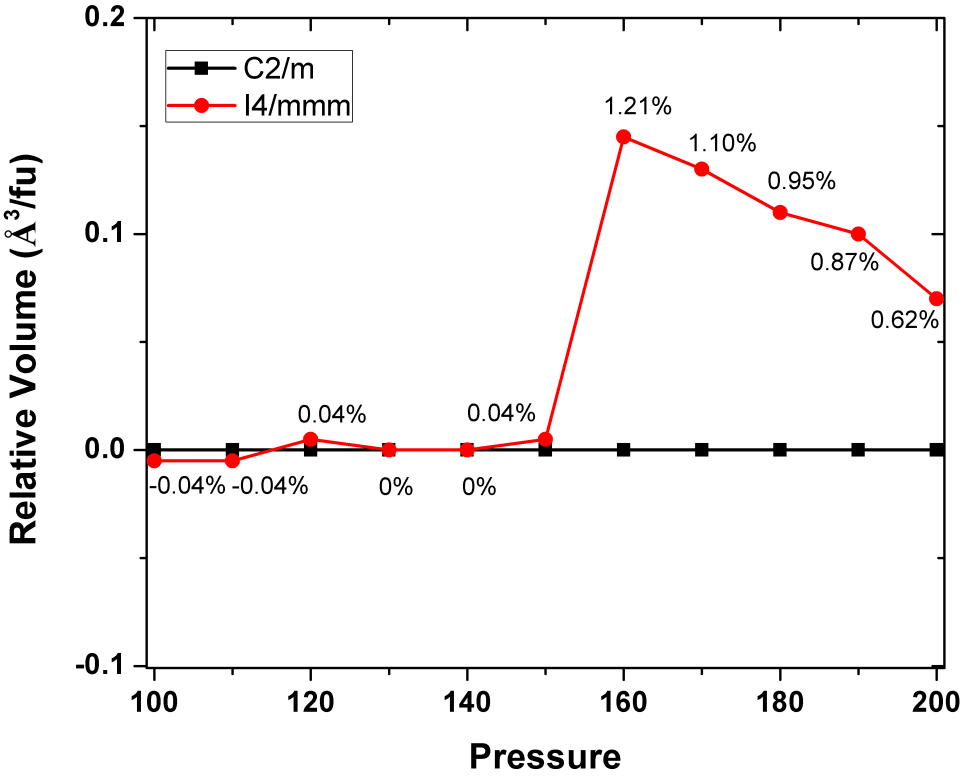

Figure S5: Comparison of relative volumes of $I4/mmm$ and 2FU-$C2/m$ phases in the pressure range between 100 and 200 GPa. The volume difference percentages ($\%V_d$) with respect to the calculated volume of 2FU-$C2/m$ ($V_{C2/m}$) is labeled for each data point of $I4/mmm$ phases ($V_{I4/mmm}$), and it is calculated by: $\%V_d = \left(\frac{V_{I4/mmm} - V_{C2/m}}{V_{C2/m}}\right) \times 100\%$

8 Electronic Band Structures and Electronic Densities of States of High Pressure PH_2 Phases

8.1 150 GPa 5FU-*C2/m*

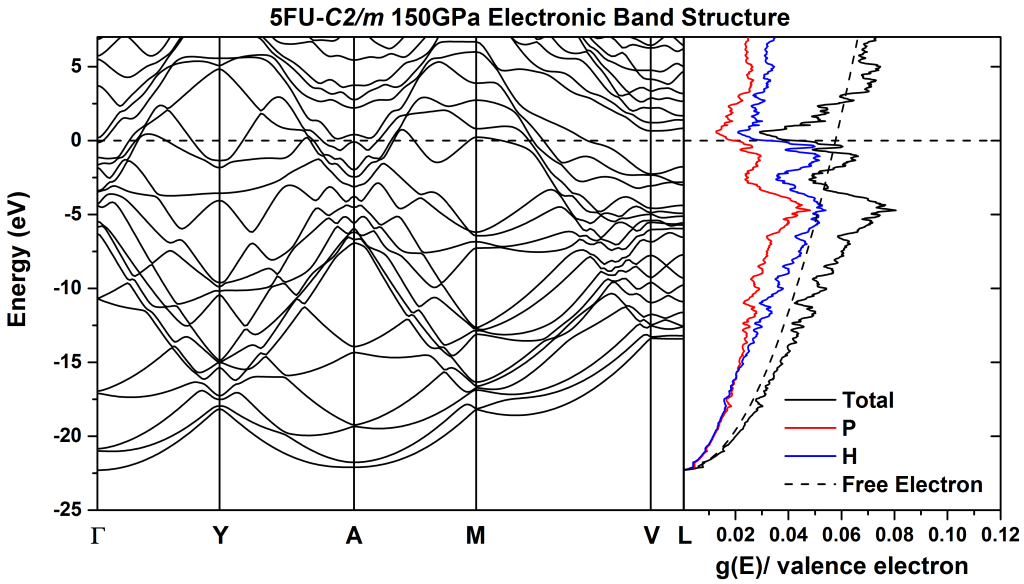

Figure S6: Electronic band structure and electronic densities of states of the 5FU-*C2/m* phase at 150 GPa.

8.2 200 GPa 5FU-*C2/m*

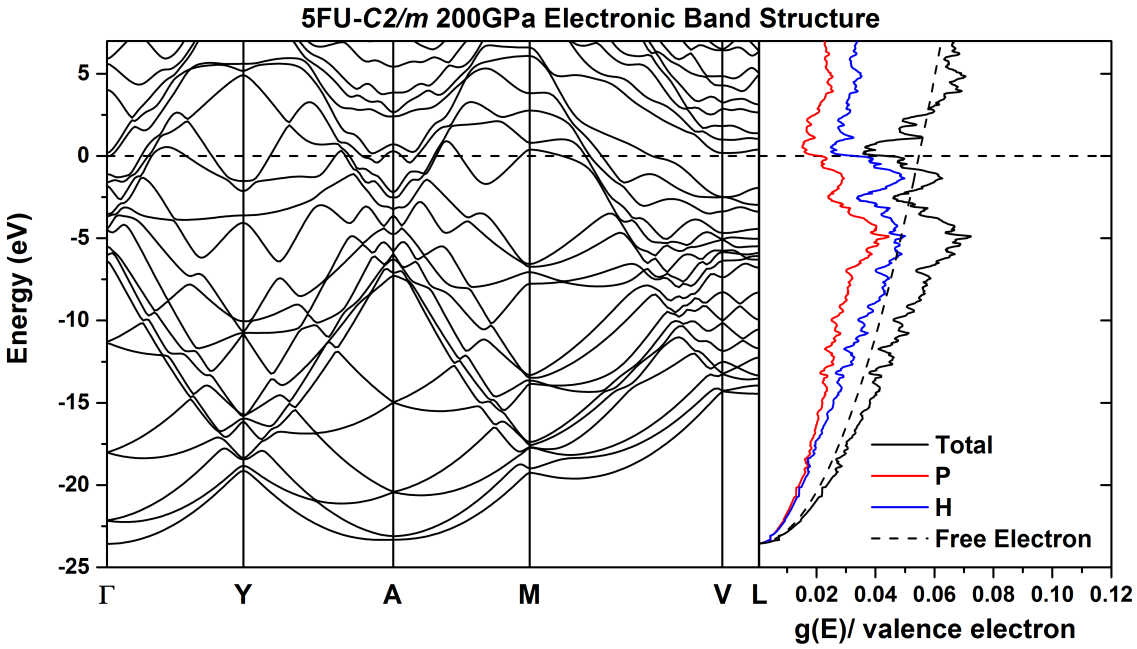

Figure S7: Electronic band structure and electronic densities of states of the 5FU-*C2/m* phase at 200 GPa.

8.3 100 GPa 2FU-*C2/m*

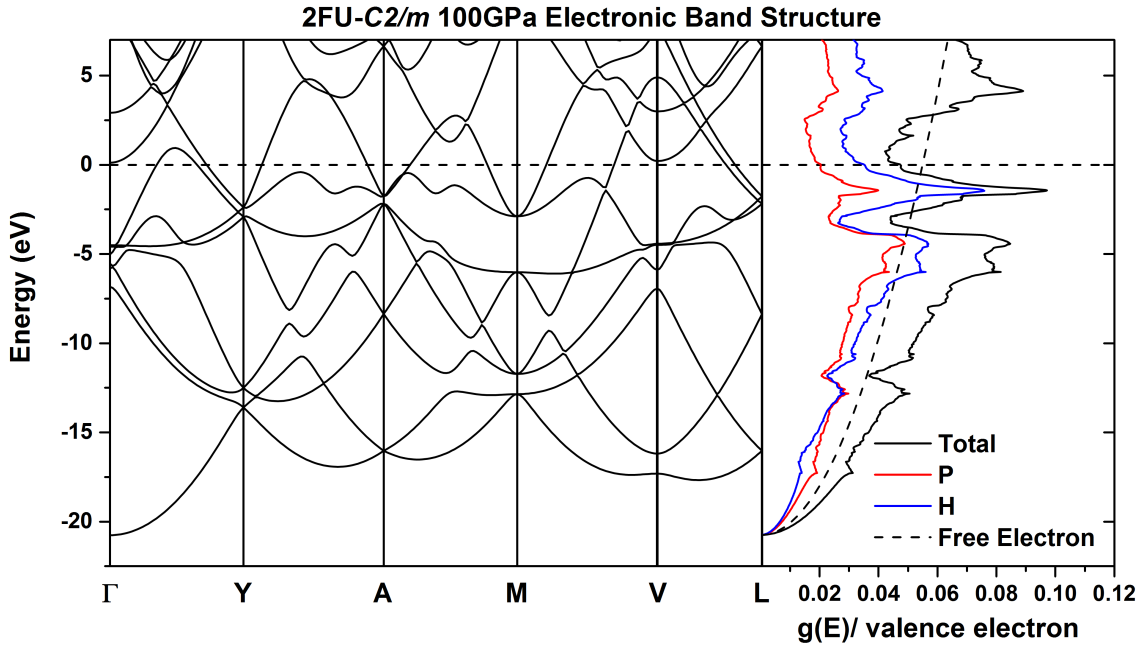

Figure S8: Electronic band structure and electron densities of state of the 2FU-*C2/m* phase at 100 GPa.

8.4 150 GPa 2FU-*C2/m*

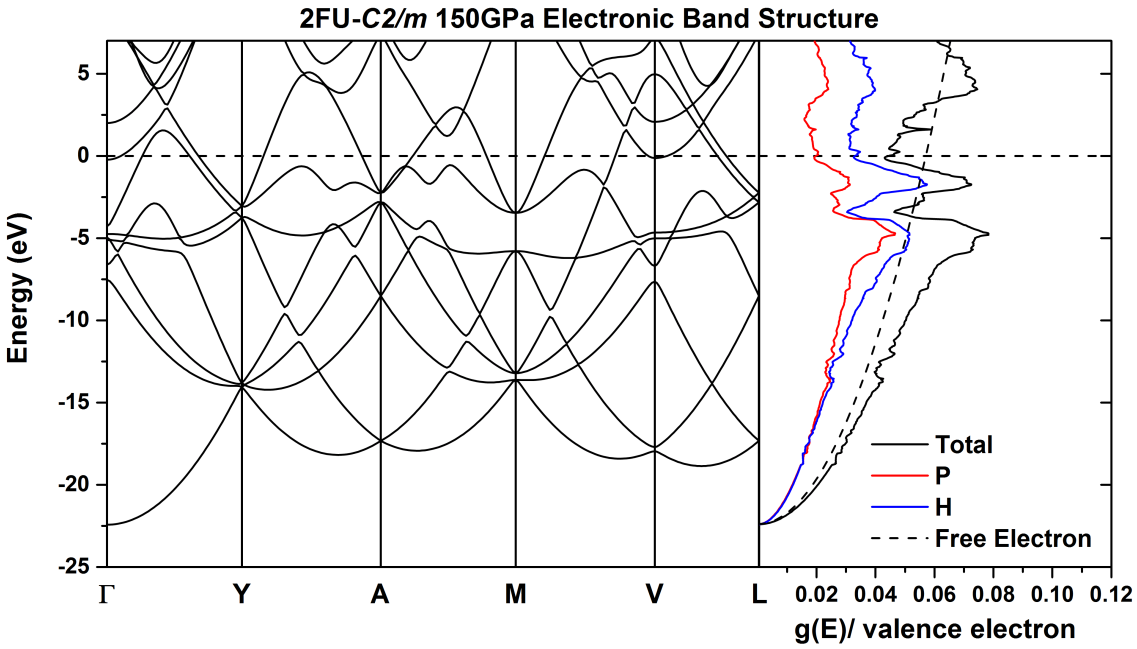

Figure S9: Electronic band structure and electronic densities of states of the 2FU-*C2/m* phase at 150 GPa.

8.5 100 GPa *I4/mmm*

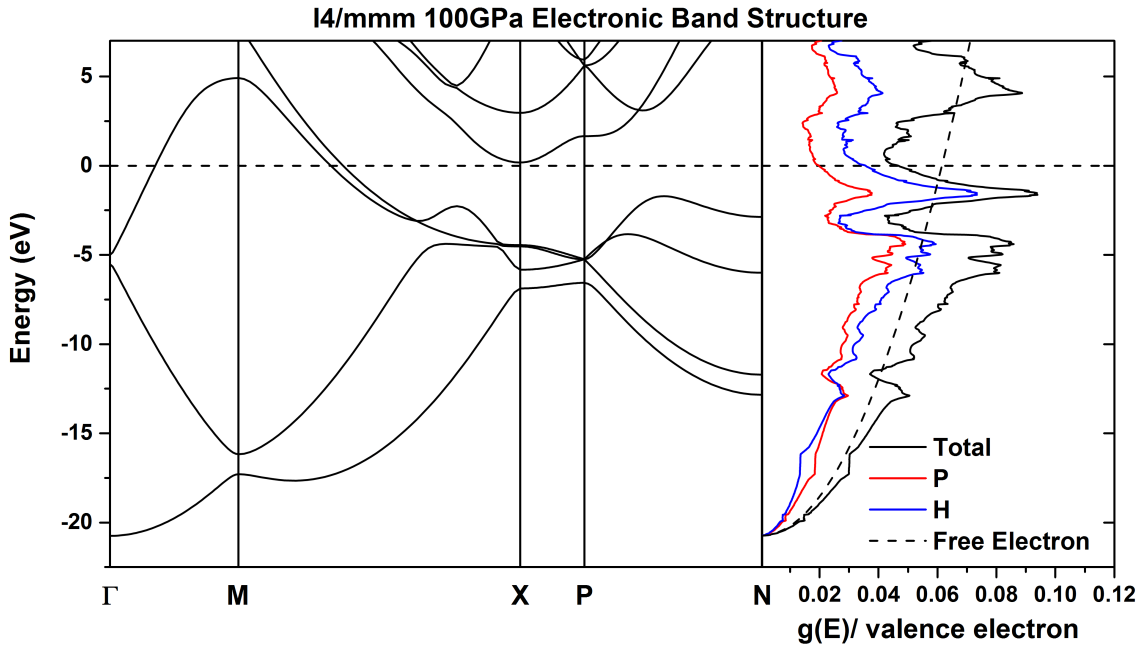

Figure S10: Electronic band structure and electronic densities of states of the *I4/mmm* phase at 100 GPa.

8.6 150 GPa *I4/mmm*

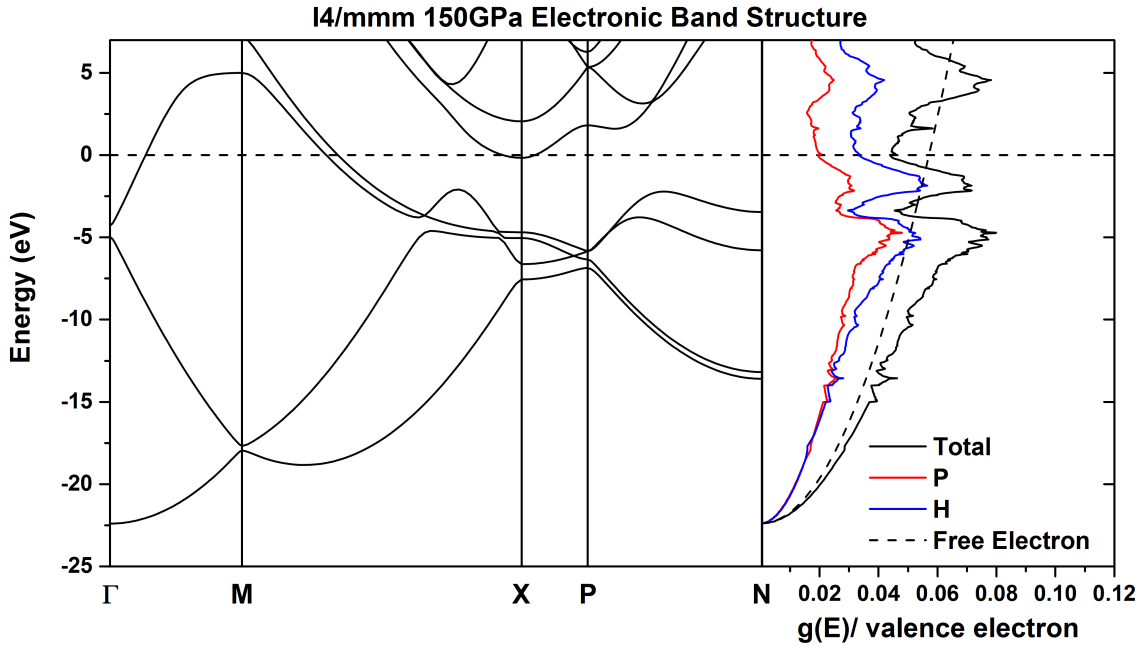

Figure S11: Electronic band structure and electronic densities of states of the *I4/mmm* phase at 150 GPa.

9 Phonon DOS, Eliashberg Spectral Function ($\alpha^2F(\omega)$) and the Electron-Phonon Integral ($\lambda(\omega)$) of High Pressure PH_2 Phases

9.1 Phonon Calculation Convergence Test

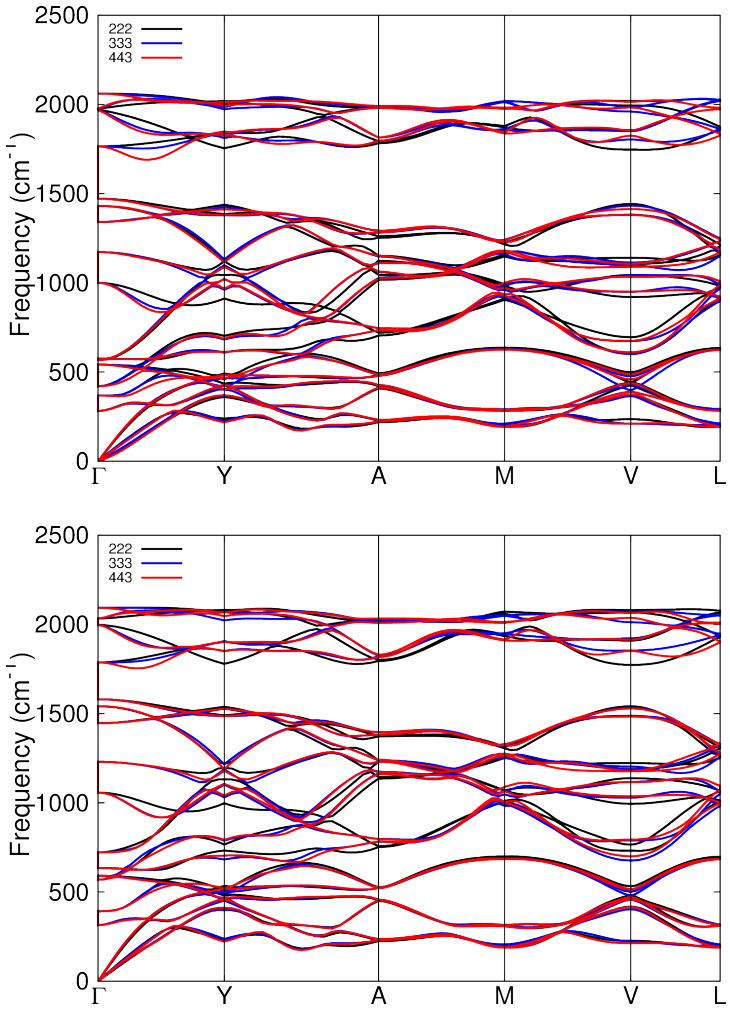

Figure S12: Phonon band structures of the 2FU-$C2/m$ phase calculated using the k-meshes given in the inset at (top) 150 GPa and (bottom) 200 GPa.

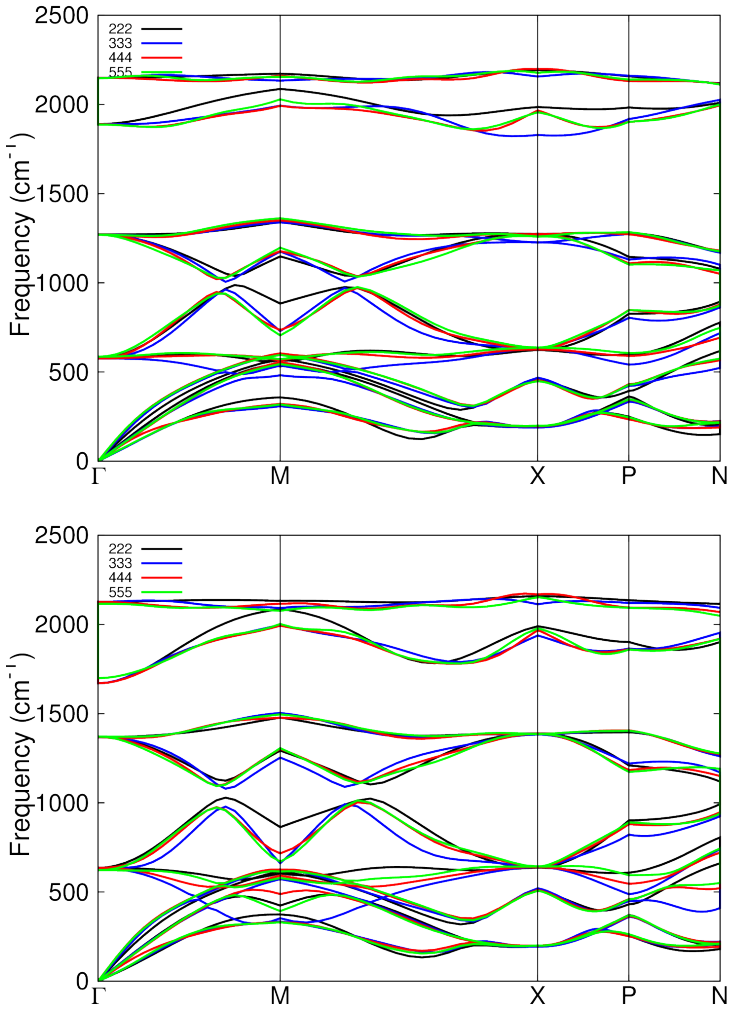

Figure S13: Phonon band structures of the $I4/mmm$ phase calculated using the k-meshes given in the inset at (top) 150 GPa and (bottom) 200 GPa.

9.2 100 GPa 5FU-*C2/m*

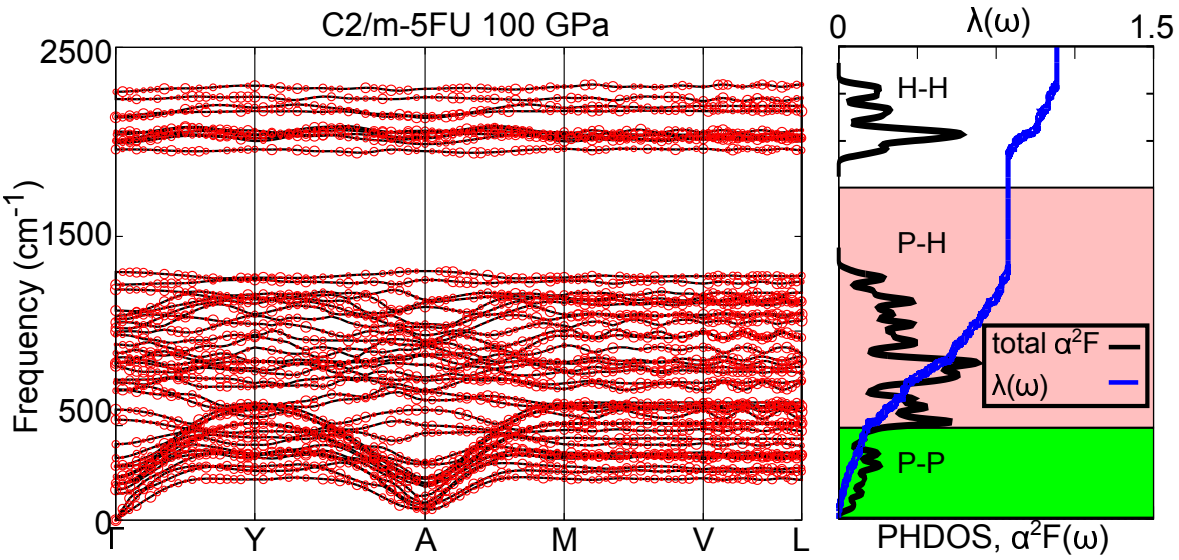

Figure S14: Phonon band structure, Eliashberg spectral function, $\alpha^2F(\omega)$, and the electron-phonon integral, $\lambda(\omega)$, for 5FU-$C2/m$ at 100 GPa. The highlighted sections of the $\alpha^2F(\omega)$ plots show the division into vibrational modes that are comprised of phosphorus vibrations (P-P, green), motions of hydrogen and phosphorus atoms (P-H, pink), and mainly hydrogen vibrations (H-H, white). The contribution towards λ for these divisions are 0.14 (13.4%), 0.67 (64.3%), and 0.23 (22.3%), for the green, pink, and white divisions, respectively. Circles indicate the phonon linewidth with a radius proportional to the strength.

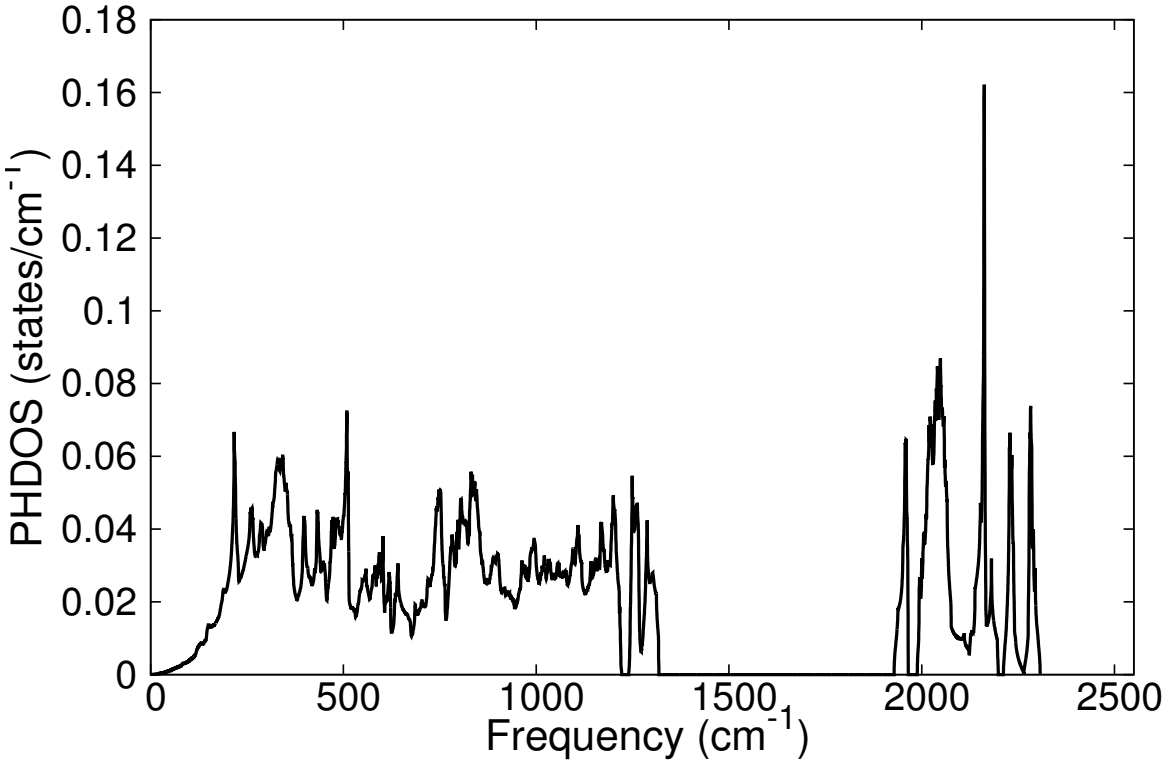

Figure S15: Phonon densities of states of the 5FU-*C2/m* phase at 100 GPa.

9.3 150 GPa 5FU-*C2/m*

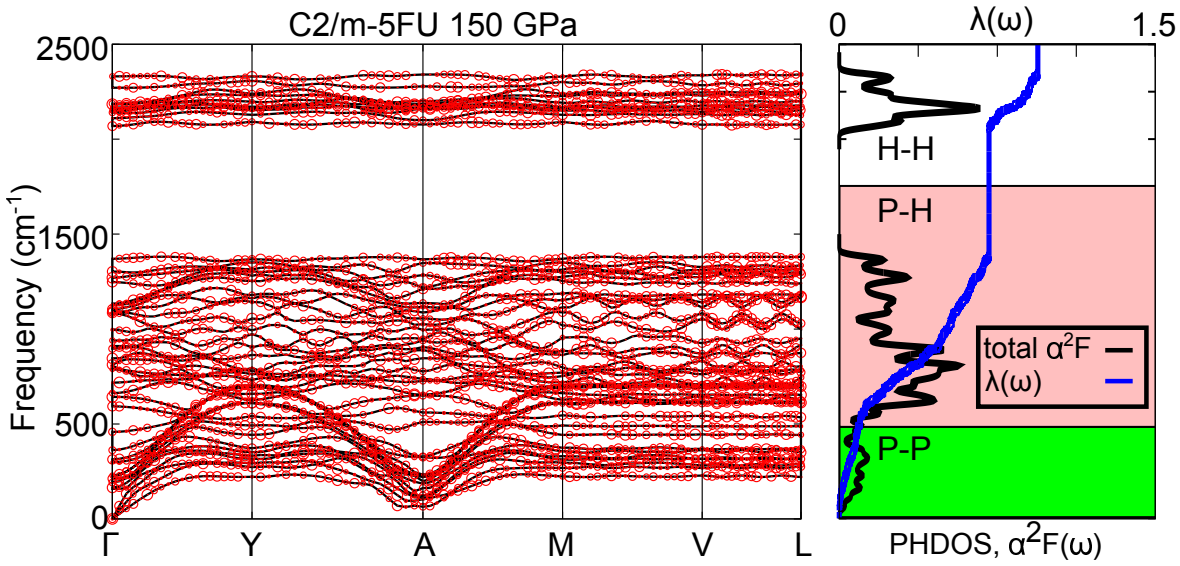

Figure S16: Phonon band structure, Eliashberg spectral function, $\alpha^2F(\omega)$, and the electron-phonon integral, $\lambda(\omega)$, for 5FU-$C2/m$ at 150 GPa. The highlighted sections of the $\alpha^2F(\omega)$ plots show the division into vibrational modes that are comprised of phosphorus vibrations (P-P, green), motions of hydrogen and phosphorus atoms (P-H, pink), and mainly hydrogen vibrations (H-H, white). The contribution towards λ for these divisions are 0.10 (10.4%), 0.61 (65.0%), and 0.23 (24.6%), for the green, pink, and white divisions, respectively. Circles indicate the phonon linewidth with a radius proportional to the strength.

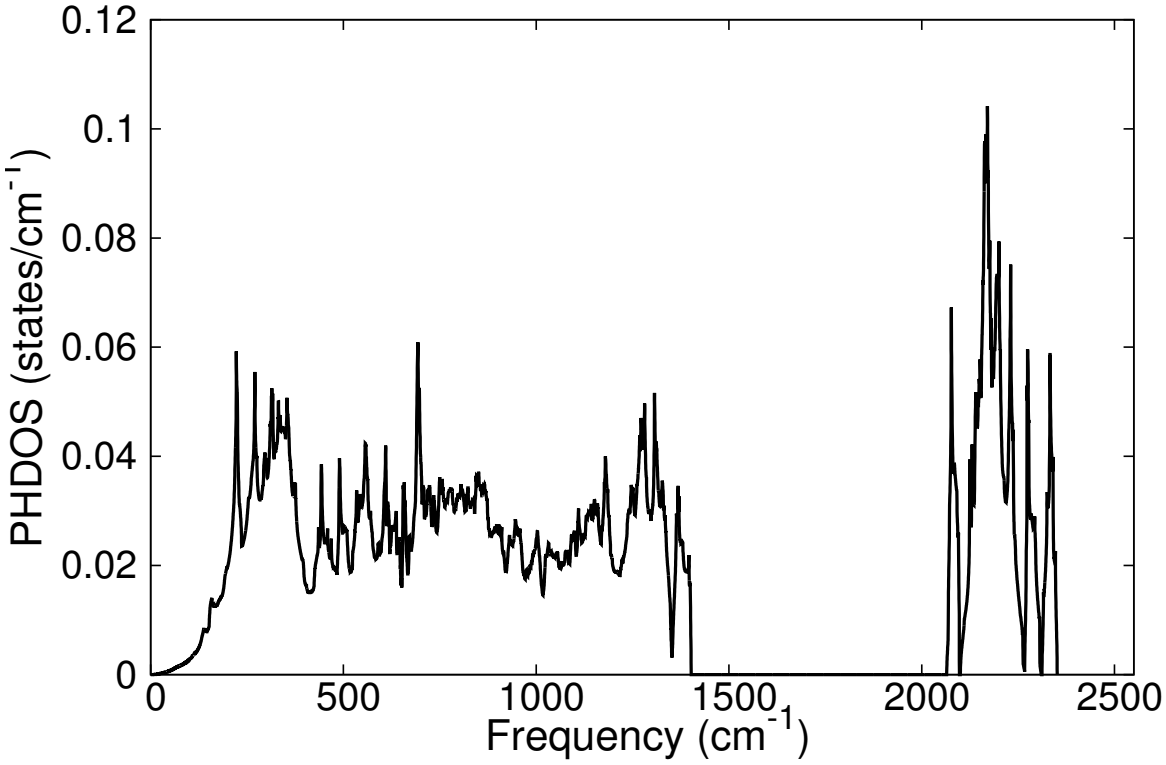

Figure S17: Phonon densities of states of the 5FU-*C2/m* phase at 150 GPa.

9.4 100 GPa 2FU-*C2/m*

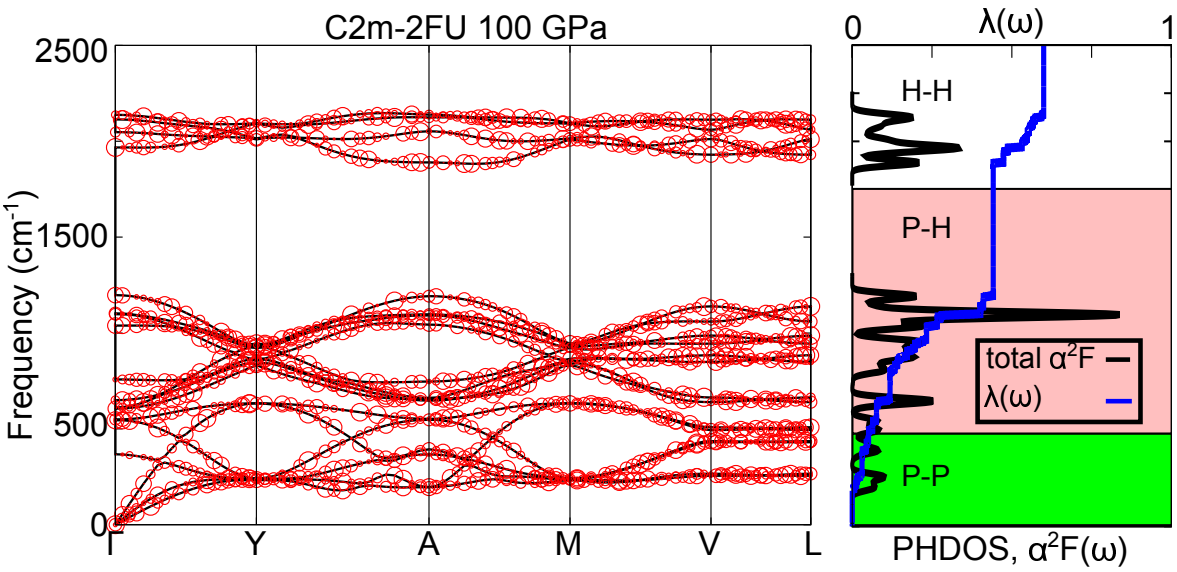

Figure S18: Phonon band structure, Eliashberg spectral function, $\alpha^2F(\omega)$, and the electron-phonon integral, $\lambda(\omega)$, for 2FU-$C2/m$ at 100 GPa. The highlighted sections of the $\alpha^2F(\omega)$ plots show the division into vibrational modes that are comprised of phosphorus vibrations (P-P, green), motions of hydrogen and phosphorus atoms (P-H, pink), and mainly hydrogen vibrations (H-H, white). The contribution towards λ for these divisions are 0.06 (9.3%), 0.39 (64.3%), and 0.16 (26.3%), for the green, pink, and white divisions, respectively. Circles indicate the phonon linewidth with a radius proportional to the strength.

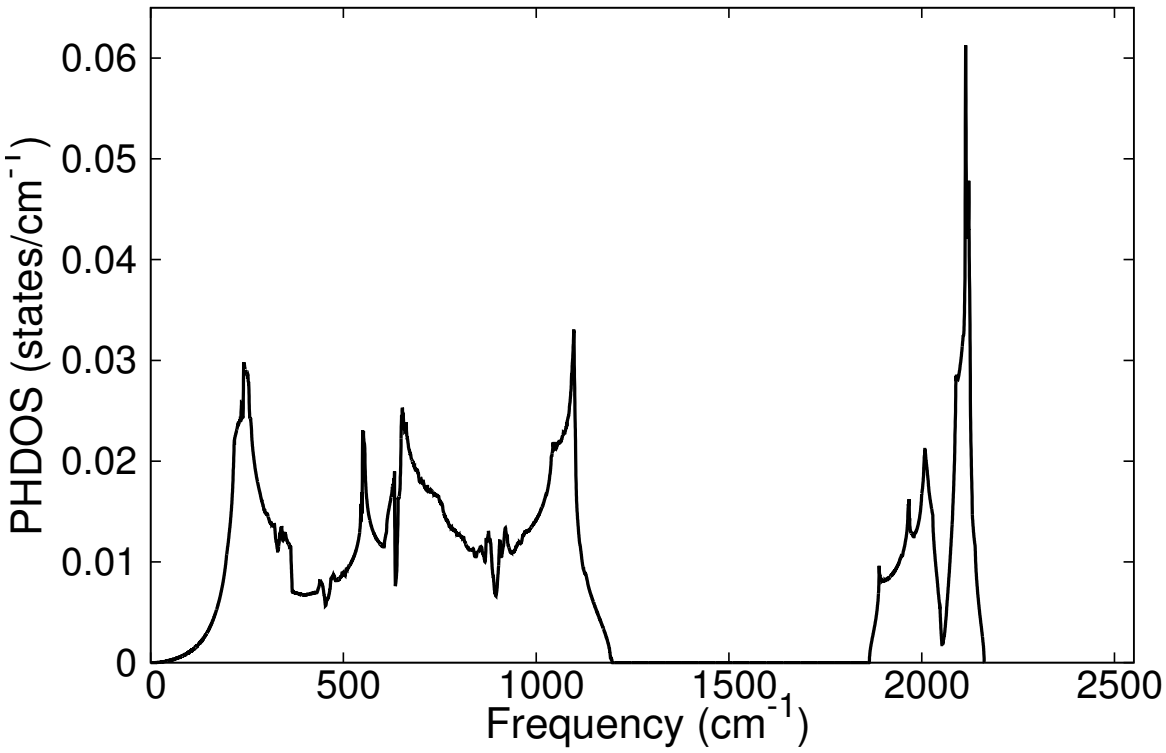

Figure S19: Phonon densities of states of the 2FU-*C2/m* phase at 10 0 GPa.

9.5 150 GPa 2FU-*C2/m*

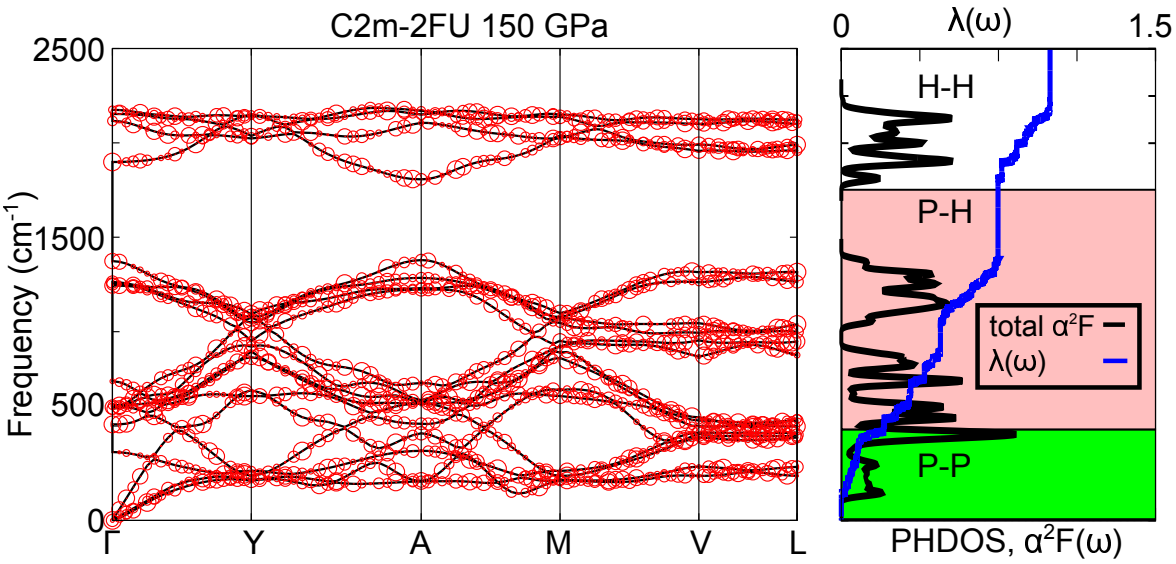

Figure S20: Phonon band structure, Eliashberg spectral function, $\alpha^2F(\omega)$, and the electron-phonon integral, $\lambda(\omega)$, for 2FU-$C2/m$ at 150 GPa. The highlighted sections of the $\alpha^2F(\omega)$ plots show the division into vibrational modes that are comprised of phosphorus vibrations (P-P, green), motions of hydrogen and phosphorus atoms (P-H, pink), and mainly hydrogen vibrations (H-H, white). The contribution towards λ for these divisions are 0.20 (20.0%), 0.55 (54.3%), and 0.26 (25.7%), for the green, pink, and white divisions, respectively. Circles indicate the phonon linewidth with a radius proportional to the strength.

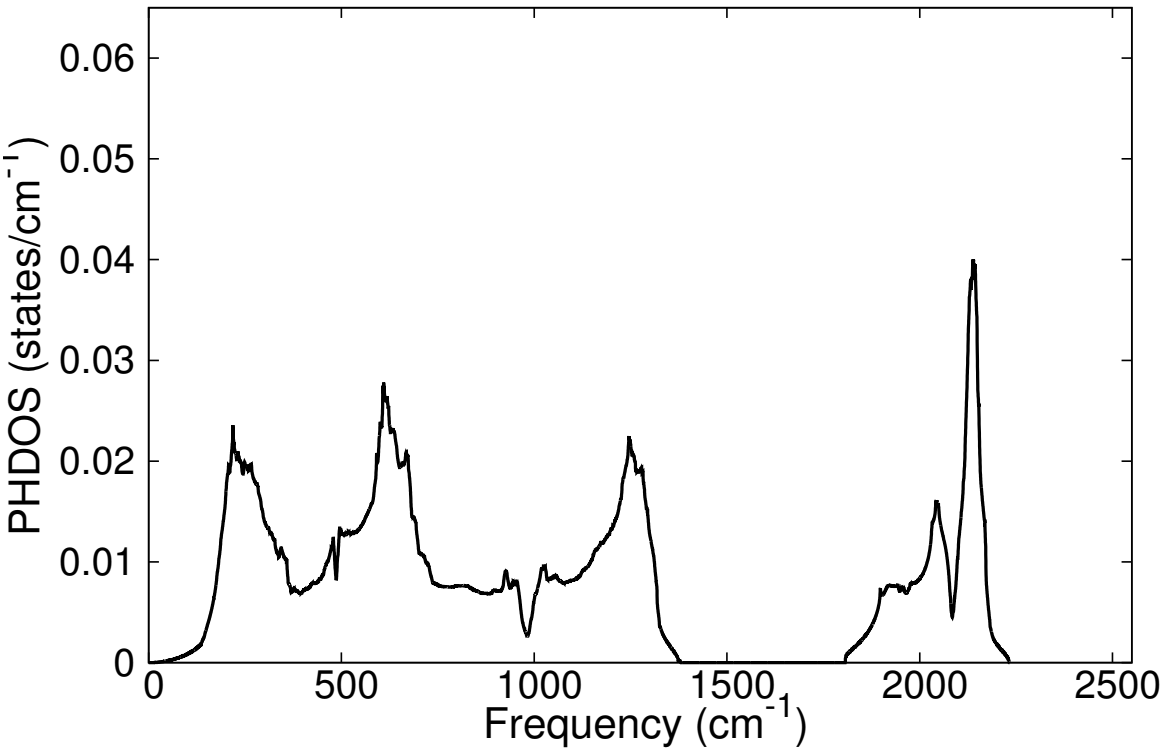

Figure S21: Phonon densities of states of the 2FU-*C2/m* phase at 150 GPa.

9.6 200 GPa 2FU-*C2/m*

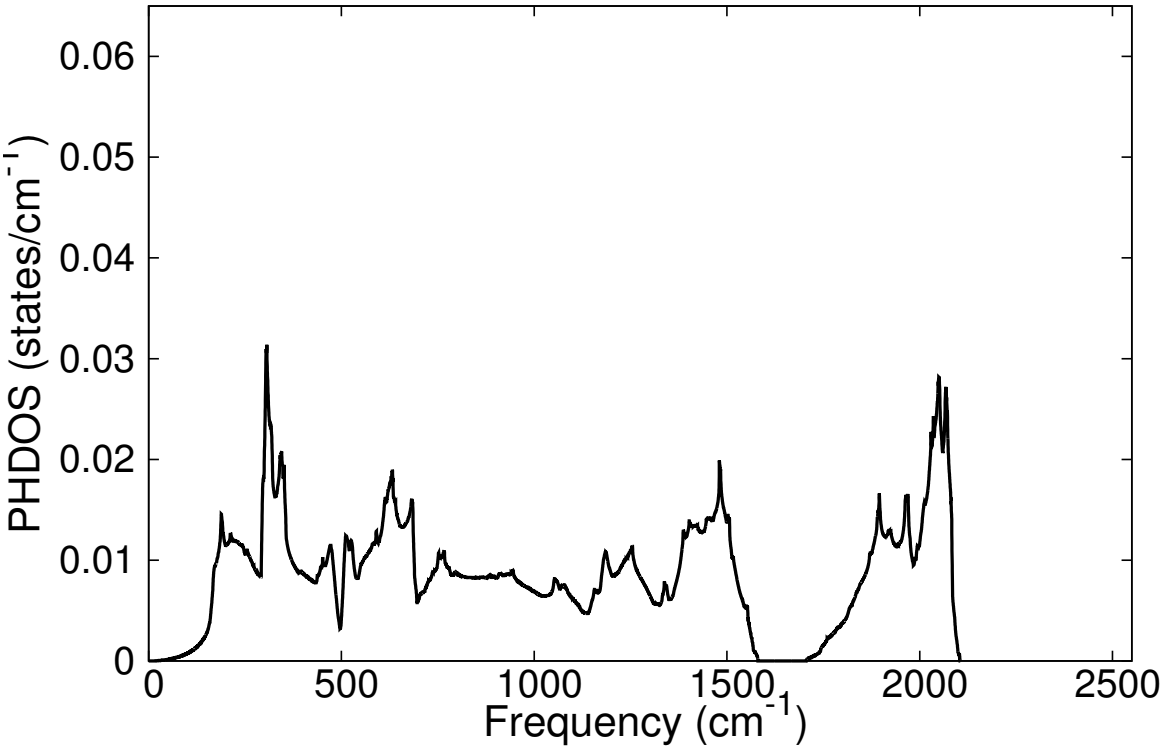

Figure S22: Phonon densities of states of the 2FU-*C2/m* phase at 200 GPa.

9.7 100 GPa *I4/mmm*

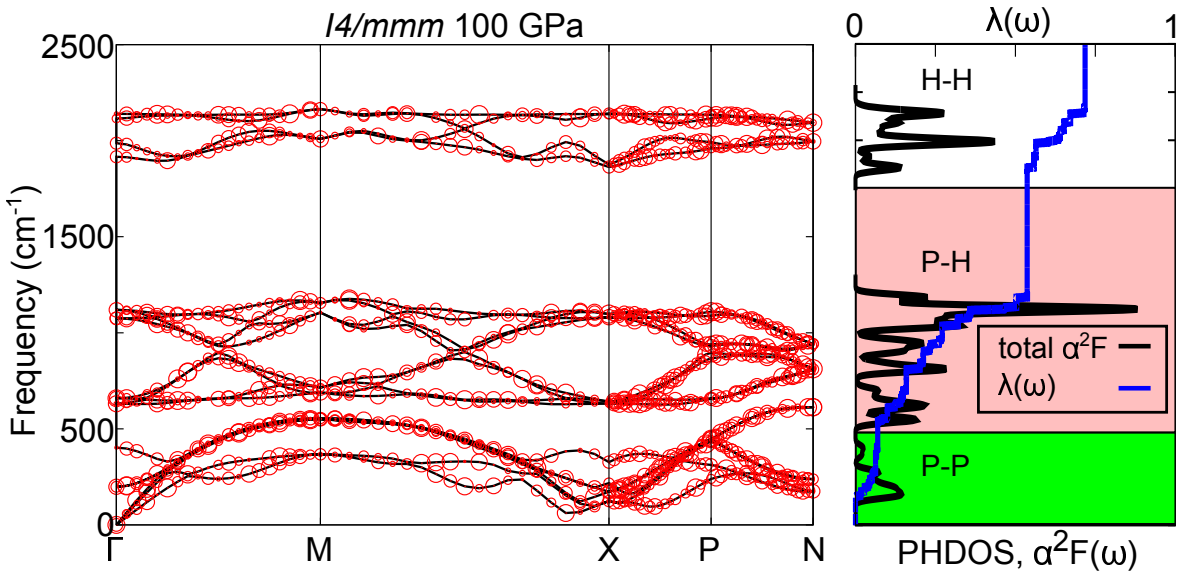

Figure S23: Phonon band structure, Eliashberg spectral function, $\alpha^2F(\omega)$, and the electron-phonon integral, $\lambda(\omega)$, for $I4/mmm$ at 100 GPa. The highlighted sections of the $\alpha^2F(\omega)$ plots show the division into vibrational modes that are comprised of phosphorus vibrations (P-P, green), motions of hydrogen and phosphorus atoms (P-H, pink), and mainly hydrogen vibrations (H-H, white). The contribution towards λ for these divisions are 0.07 (9.7%), 0.47 (65.1%), and 0.18 (25.2%), for the green, pink, and white divisions, respectively. Circles indicate the phonon linewidth with a radius proportional to the strength.

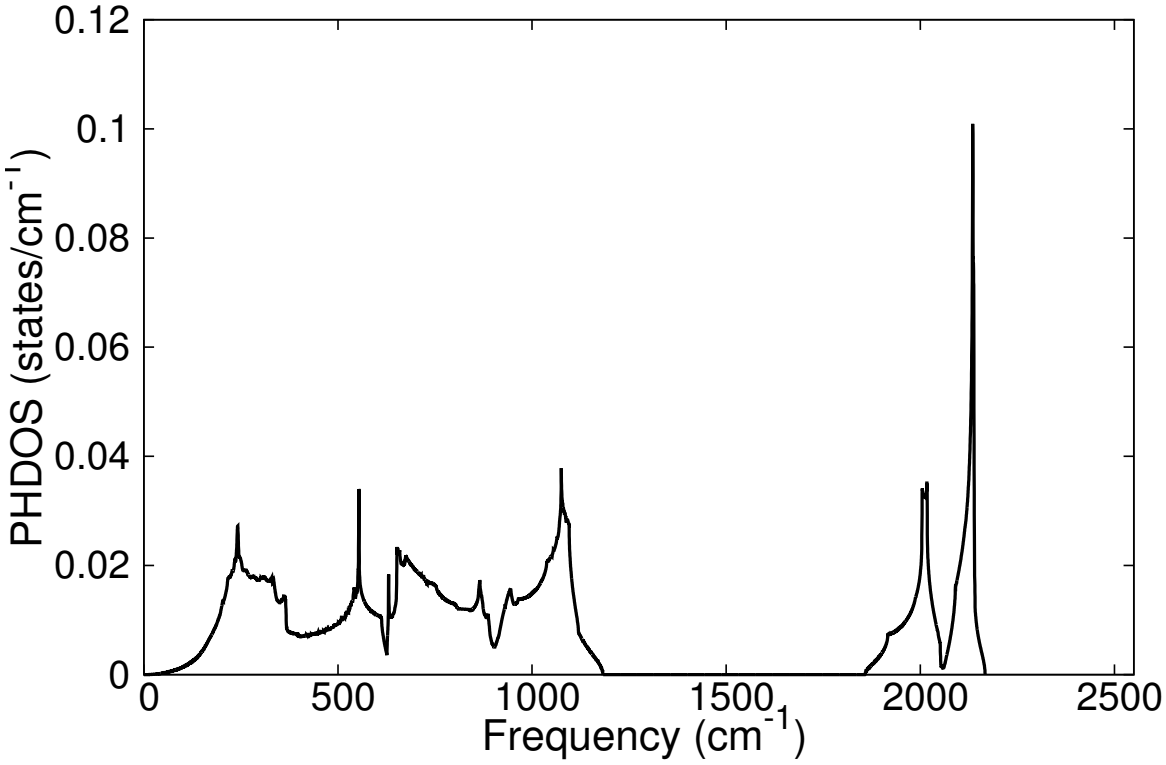

Figure S24: Phonon densities of states of the *I4/mmm* phase at 100 GPa.

9.8 150 GPa *I4/mmm*

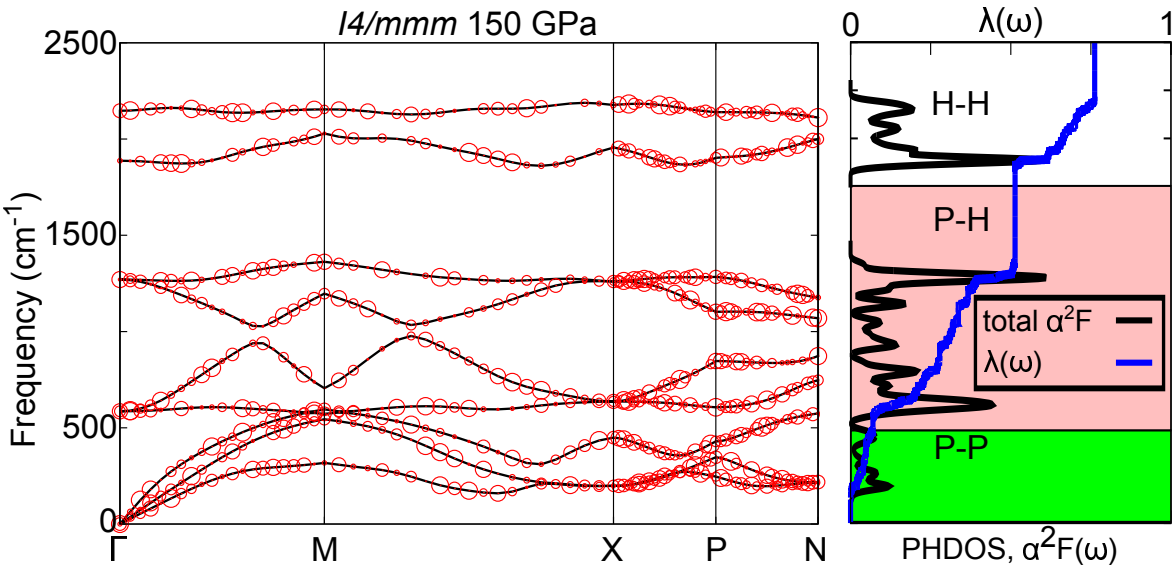

Figure S25: Phonon band structure, Eliashberg spectral function, $\alpha^2F(\omega)$, and the electron-phonon integral, $\lambda(\omega)$, for $I4/mmm$ at 150 GPa. The highlighted sections of the $\alpha^2F(\omega)$ plots show the division into vibrational modes that are comprised of phosphorus vibrations (P-P, green), motions of hydrogen and phosphorus atoms (P-H, pink), and mainly hydrogen vibrations (H-H, white). The contribution towards λ for these divisions are 0.07 (9.2%), 0.44 (58.2%), and 0.25 (32.6%), for the green, pink, and white divisions, respectively. Circles indicate the phonon linewidth with a radius proportional to the strength.

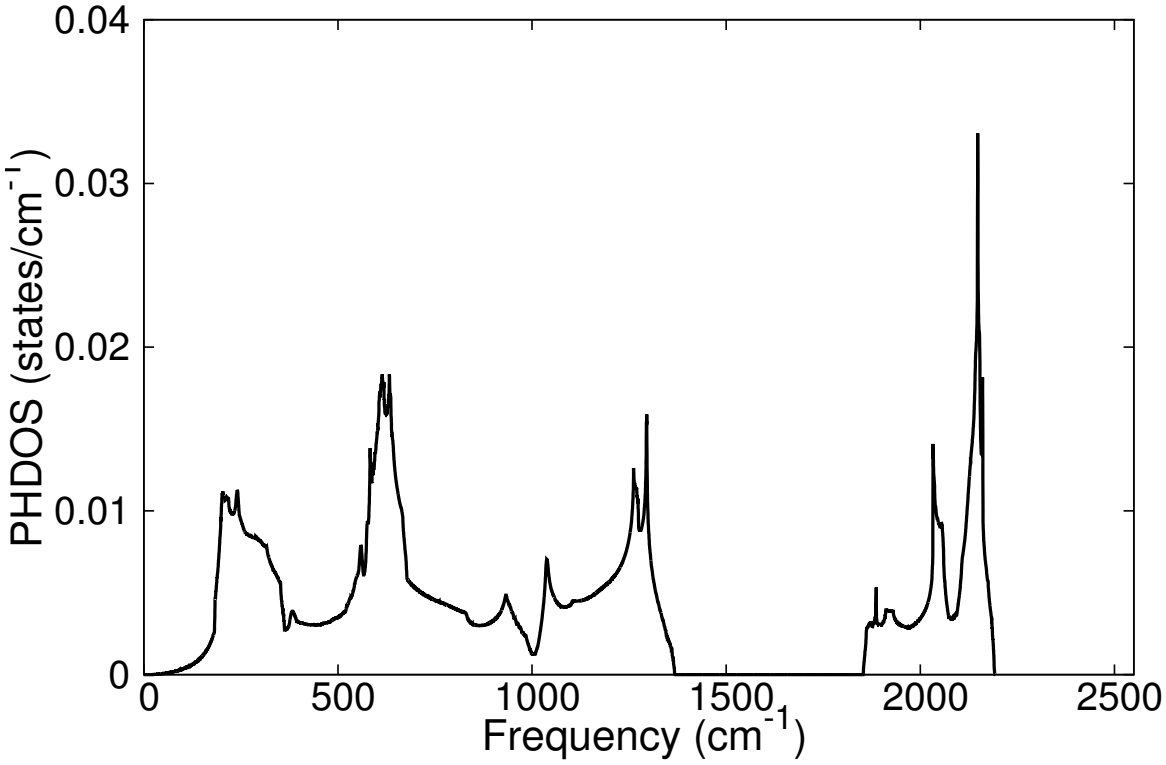

Figure S26: Phonon densities of states of the *I4/mmm* phase at 150 GPa.

9.9 200 GPa *I4/mmm*

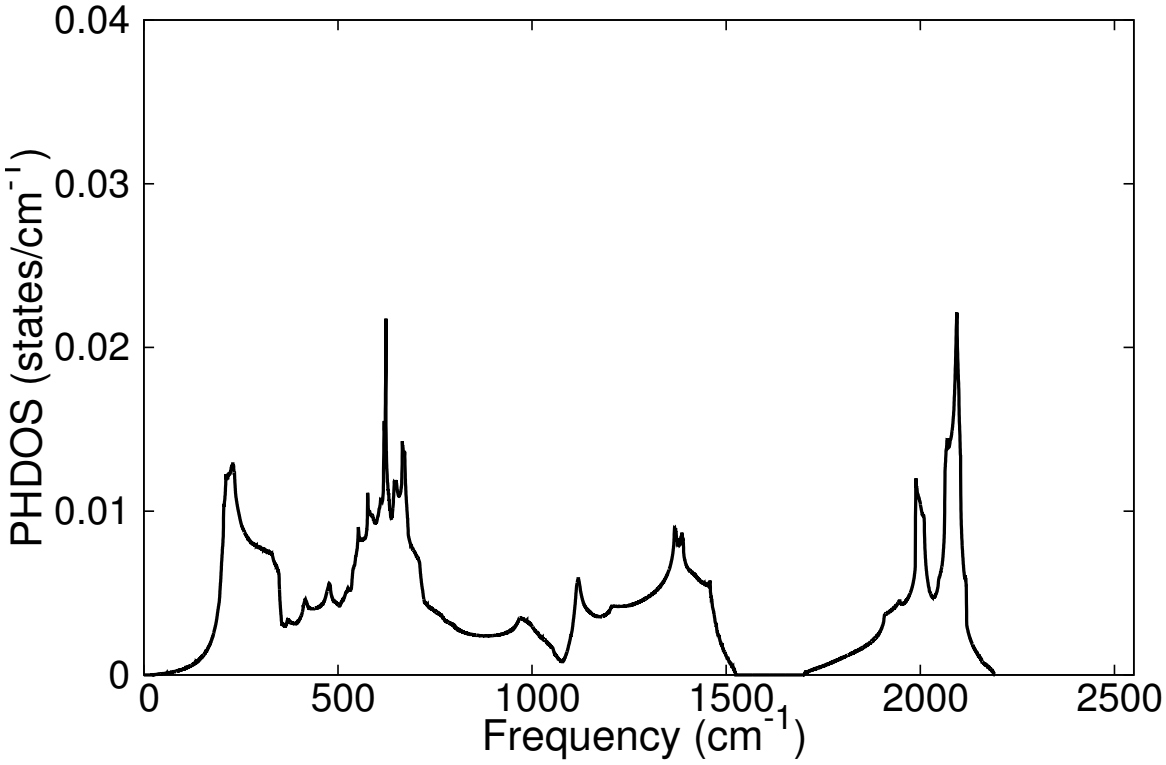

Figure S27: Phonon densities of states of the *I4/mmm* phase at 200 GPa.

9.10 T_cs of 5FU-*C2/m*, 2FU-*C2/m* and *I4/mmm*

Structure	**Pressure**	**T_c (K)**					
	(GPa)	μ^* = 0.10	0.12	0.14	0.16	0.18	0.20
5FU-$C2/m$	100	49.01	44.64	40.35	36.17	32.10	28.19
	150	55.52	50.24	45.08	40.07	35.24	30.61
5FU-$C2/m$	100	35.55	29.95	24.73	19.96	15.67	11.89
	150	61.45	56.24	51.12	46.10	41.21	36.48
	200	75.59	68.75	62.04	55.51	49.18	43.08
$I4/mmm$	100	32.47	27.85	23.50	19.45	15.74	12.40
	150	50.60	44.65	38.93	33.49	28.35	23.55
	200	70.36	64.62	58.97	53.42	48.00	42.73

Table S17: Calculated T_cs of 5FU-*C2/m*, 2FU-*C2/m* and *I4/mmm* at various pressures with μ^* = 0.10, 0.12, 0.14, 0.16, 0.18 and 0.20.

10 Electron Localization Functions of High Pressure PH_2 Phases

10.1 100 GPa 5FU-*C2/m*

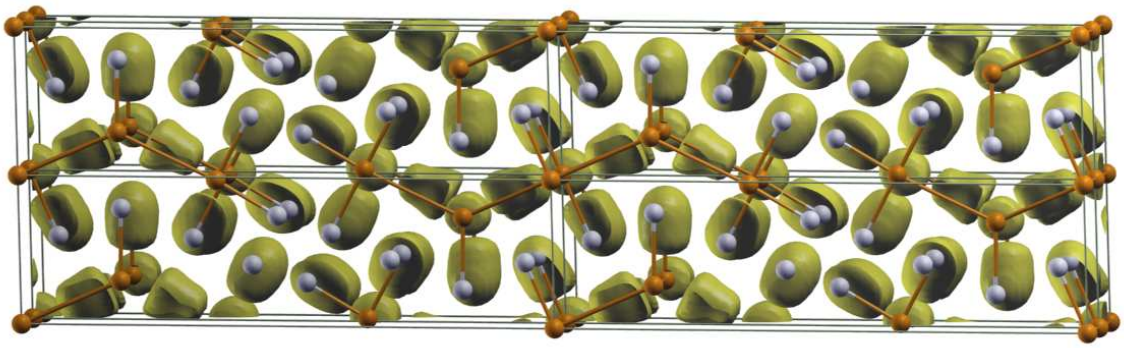

Figure S28: An isosurface (ELF = 0.7) of the electron localization function of the 5FU-*C2/m* PH_2 phase at 100 GPa.

10.2 200 GPa 2FU-*C2/m*

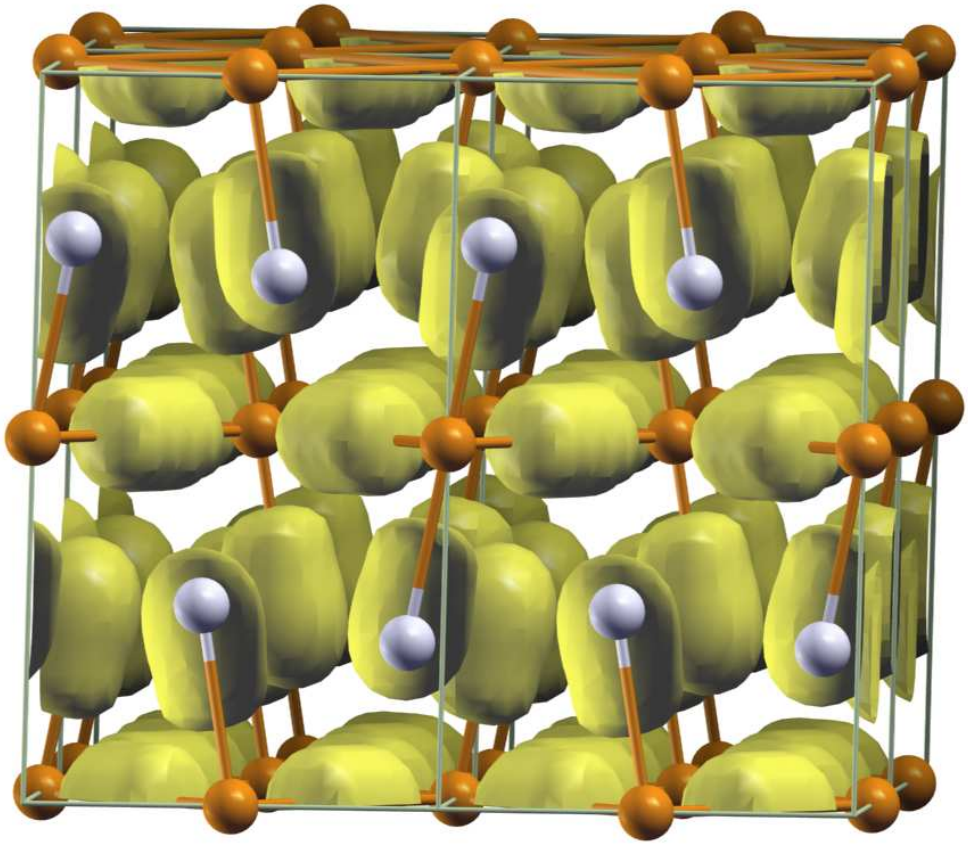

Figure S29: An isosurface (ELF = 0.7) of the electron localization function of the 2FU-*C2/m* PH_2 phase at 200 GPa.

10.3 200 GPa *I4/mmm*

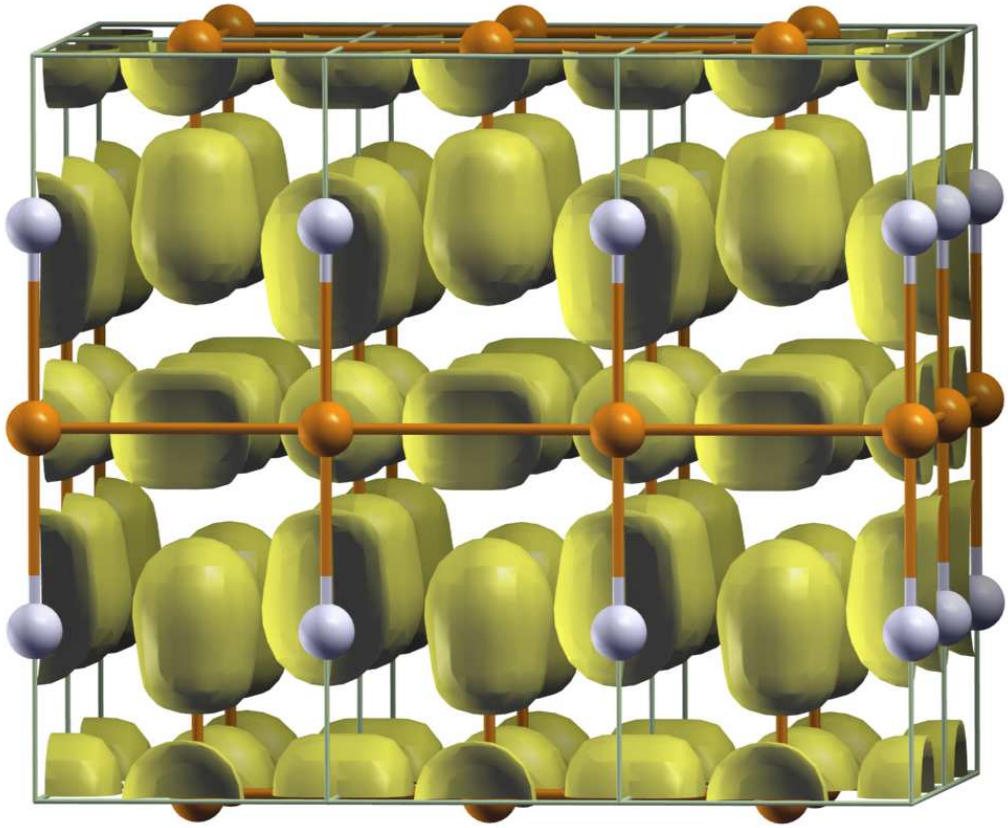

Figure S30: An isosurface (ELF = 0.7) of the electron localization function of the *I4/mmm* PH_2 phase at 200 GPa.

11 Zone-center Vibrational Frequencies of High Pressure PH_2 Phases

11.1 100 GPa 5FU-*C2/m*

The zone-center vibrational frequencies in cm^{-1} at 100 GPa are: 43.5 (I), 52.4 (I), 55.6 (I), 140.0 (R), 160.3 (R), 185.7 (I), 193.5 (I), 225.2 (R), 230.0 (I), 281.4 (I), 287.4 (R), 328.7 (R), 401.8 (I), 531.0 (R), 587.2 (I), 668.5 (I), 681.6 (I), 723.1 (I), 742.1 (R), 814.3 (R), 826.8 (I), 832.5 (R), 856.7 (I), 882.9 (I), 929.0 (R), 980.2 (R), 996.7 (R), 1016.6 (I), 1045.3 (r), 1062.8 (R), 1075.7 (I), 1108.1 (I), 1219.5 (R), 1246.3 (I), 1311.8 (R), 1958.8 (I), 1992.8 (R), 2000.9 (I), 2006.3 (R), 2039.1 (R), 2055.7 (I), 2130.1 (R), 2134.4 (I), 2223.3 (I), 2264.8 (R).

11.2 150 GPa 5FU-*C2/m*

The zone-center vibrational frequencies in cm^{-1} at 150 GPa are: 45.4 (I), 52.5 (I), 56.4 (I), 158.2 (R), 164.8 (R), 190.5 (I), 211.2 (I), 226.5 (R), 228.7 (I), 296.3 (I), 313.7 (R), 362.1 (R), 458.5 (I), 592.9 (R), 648.1 (I), 651.4 (I), 698.6 (I), 779.8 (I), 807.0 (I), 812.1 (R), 845.9 (R), 892.7 (I), 910.5 (R), 939.8 (I), 996.4 (R), 1078.9 (R), 1085.8 (R), 1093.6 (I), 1103.4 (I), 1124.9 (R), 1133.8 (R), 1248.0 (I), 1270.3 (R), 1302.9 (I), 1369.9 (R), 2064.4 (I), 2110.3 (R), 2140.2 (R), 2140.9 (I), 2155.1 (I), 2166.7 (R), 2183.8 (R), 2187.8 (I), 2267.0 (I), 2330.7 (R).

11.3 100 GPa 2FU-*C2/m*

The zone-center vibrational frequencies in cm^{-1} at 100 GPa are: 21.4 (I), 22.3 (I), 29.6 (I), 367.2 (I), 545.0 (I), 549.7 (I), 608.8 (I), 614.2 (I), 649.5 (R), 757.5 (I), 1038.6 (R), 1098.3 (R), 1102.5 (R), 1197.3 (I), 1968.0 (R), 2047.7 (I), 2111.9 (I), 2138.2 (R).

11.4 150 GPa 2FU-*C2/m*

The zone-center vibrational frequencies in cm^{-1} at 150 GPa are: 22.5 (I), 25.7 (I), 42.8 (I), 361.8 (I), 508.6 (R), 593.3 (I), 600.4 (I), 608.3 (I), 609.6 (I), 737.0 (I), 1244.5 (R), 1251.0 (R), 1262.7 (R), 1373.6 (I), 1898.6 (R), 2116.4 (I), 2143.4 (I), 2175.1 (R).

11.5 200 GPa 2FU-*C2/m*

The zone-center vibrational frequencies in cm^{-1} at 200 GPa are: 16.7 (I), 21.9 (I), 30.9 (I), 315.6 (I), 392.4 (I), 558.9 (I), 592.0 (I), 634.5 (I), 721.7 (R), 1057.5 (I), 1229.9 (R), 1451.7 (R), 1541.7 (R), 1578.5 (I), 1786.3 (R), 1998.2 (I), 2026.4 (R), 2090.7 (I).

11.6 100 GPa *I4/mmm*

The zone-center vibrational frequencies in cm^{-1} at 100 GPa are: 21.2 (I), 70.4 (I), 198.2 (I), 402.2 (I), 612.0 (I), 659.2 (R), 1075.3 (I), 1119.7 (R), 1916.4 (I), 1986.9 (R), 2114.8 (I), 2139.7 (R).

11.7 150 GPa *I4/mmm*

The zone-center vibrational frequencies in cm^{-1} at 150 GPa are: 18.0 (I), 23.1 (I), 599.4 (I), 1270.0 (R), 1887.2 (R), 2147.3 (I).

11.8 200 GPa *I4/mmm*

The zone-center vibrational frequencies in cm^{-1} at 200 GPa are: 25.1 (I), 53.7 (I), 615.0 (I), 1371.5 (R), 1699.0 (R), 2115.5 (I).

12 Nedged Elastic Band (NEB) Calculation (*I4/mmm* to 2FU-*C2/m*)

12.1 Calculated NEB Barrier Plot

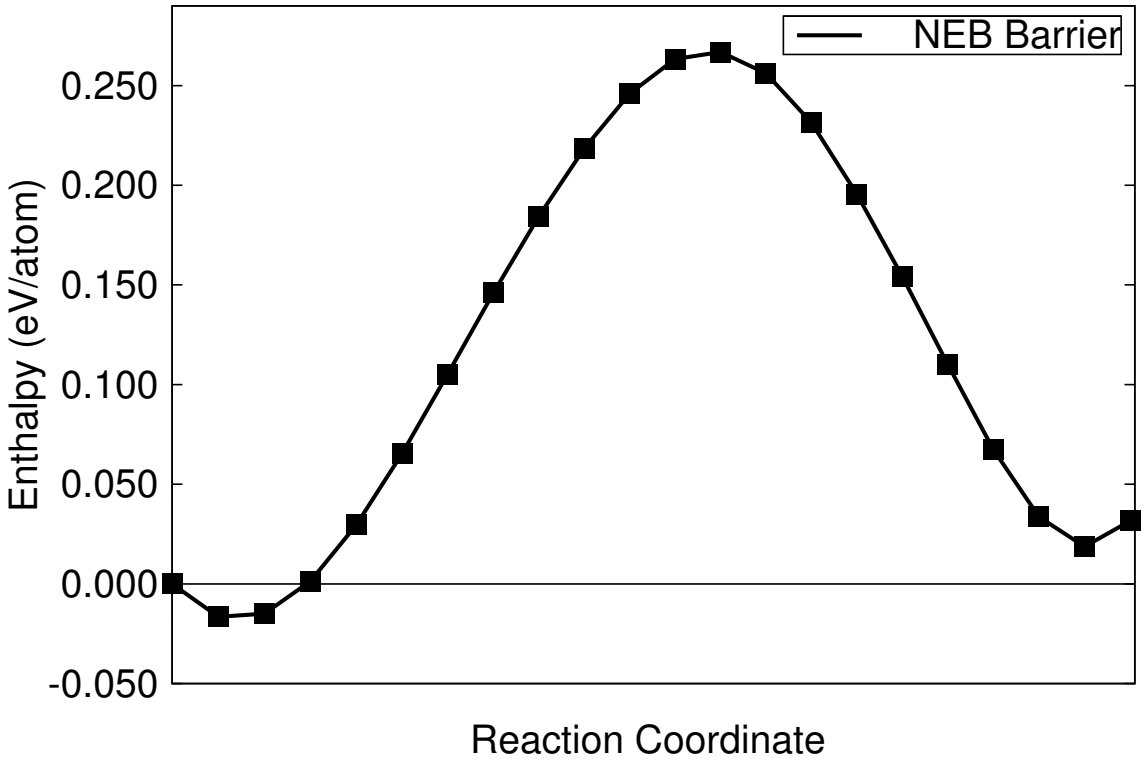

Figure S31: Calculated NEB barrier plot of individual images with enthalpies relative to the enthalpy of the starting $I4/mmm$ structure.

12.2 Stepwise Vasp POSCARs obtained in the NEB calculations

NEB-01			
H4 P2			
1.00000			
	2.07557	0.00000	0.00000
	0.00000	4.15115	0.00000
	-1.03779	-1.03779	2.63644
4 2			
Direct			
	0.77186	0.38593	0.54372
	0.22814	0.11407	0.45628
	0.77186	0.88593	0.54372
	0.22814	0.61407	0.45628
	0.50000	0.25000	0.00000
	0.50000	0.75000	0.00000

NEB-02			
H4 P2			
1.00000			
	2.11771	0.00000	0.00000
	0.00000	4.09437	0.00074
	-1.05886	-0.98972	2.63354
4 2			
Direct			
	0.76961	0.38737	0.53922
	0.22800	0.11269	0.45599
	0.77200	0.88731	0.54401
	0.23039	0.61263	0.46078
	0.50000	0.23810	0.00000
	0.52381	0.73810	0.00000

NEB-03			
H4 P2			
1.00000			
	2.15985	0.00000	0.00000
	0.00000	4.03759	0.00148
	-1.07992	-0.94166	2.63064
4 2			
Direct			
	0.76736	0.38880	0.53471
	0.22785	0.11131	0.45570
	0.77215	0.88869	0.54430
	0.23264	0.61120	0.46529
	0.50000	0.22619	0.00000
	0.54762	0.72619	0.00000

NEB-04			
H4 P2			
1.00000			
	2.20199	0.00000	0.00000
	0.00000	3.98082	0.00223
	-1.10099	-0.89359	2.62774
4 2			
Direct			
	0.76511	0.39024	0.53021
	0.22771	0.10994	0.45541
	0.77229	0.89006	0.54459
	0.23489	0.60976	0.46979
	0.50000	0.21429	0.00000
	0.57143	0.71429	0.00000

NEB-05			
H4 P2			
1.00000			
	2.24412	0.00000	0.00000
	0.00000	3.92404	0.00297
	-1.12206	-0.84553	2.62484
4 2			
Direct			
	0.76285	0.39168	0.52571
	0.22756	0.10856	0.45512
	0.77244	0.89144	0.54488
	0.23715	0.60832	0.47429
	0.50000	0.20238	0.00000
	0.59524	0.70238	0.00000

NEB-06			
H4 P2			
1.00000			
	2.28626	0.00000	0.00000
	0.00000	3.86726	0.00371
	-1.14313	-0.79746	2.62194
4 2			
Direct			
	0.76060	0.39312	0.52121
	0.22742	0.10718	0.45484
	0.77258	0.89282	0.54516
	0.23940	0.60688	0.47879
	0.50000	0.19048	0.00000
	0.61905	0.69048	0.00000

NEB-07			
H4 P2			
1.00000			
	2.32840	0.00000	0.00000
	0.00000	3.81049	0.00445
	-1.16420	-0.74940	2.61904
4 2			
Direct			
	0.75835	0.39455	0.51670
	0.22727	0.10580	0.45455
	0.77273	0.89420	0.54545
	0.24165	0.60545	0.48330
	0.50000	0.17857	0.00000
	0.64286	0.67857	0.00000

NEB-08			
H4 P2			
1.00000			
	2.37053	0.00000	0.00000
	0.00000	3.75371	0.00519
	-1.18527	-0.70133	2.61614
4 2			
Direct			
	0.75610	0.39599	0.51220
	0.22713	0.10442	0.45426
	0.77287	0.89558	0.54574
	0.24390	0.60401	0.48780
	0.50000	0.16667	0.00000
	0.66667	0.66667	0.00000

NEB-09			
H4 P2			
1.00000			
	2.41267	0.00000	0.00000
	0.00000	3.69693	0.00593
	-1.20634	-0.65327	2.61323
4 2			
Direct			
	0.75385	0.39743	0.50770
	0.22698	0.10305	0.45397
	0.77302	0.89695	0.54603
	0.24615	0.60257	0.49230
	0.50000	0.15476	0.00000
	0.69048	0.65476	0.00000

NEB-10			
H4 P2			
1.00000			
	2.45481	0.00000	0.00000
	0.00000	3.64016	0.00668
	-1.22740	-0.60520	2.61033
4 2			
Direct			
	0.75160	0.39886	0.50319
	0.22684	0.10167	0.45368
	0.77316	0.89833	0.54632
	0.24840	0.60114	0.49681
	0.50000	0.14286	0.00000
	0.71429	0.64286	0.00000

NEB-11			
H4 P2			
1.00000			
	2.49695	0.00000	0.00000
	0.00000	3.58338	0.00742
	-1.24847	-0.55714	2.60743
4 2			
Direct			
	0.74935	0.40030	0.49869
	0.22670	0.10029	0.45339
	0.77330	0.89971	0.54661
	0.25065	0.59970	0.50131
	0.50000	0.13095	0.00000
	0.73810	0.63095	0.00000

NEB-12			
H4 P2			
1.00000			
	2.53908	0.00000	0.00000
	0.00000	3.52660	0.00816
	-1.26954	-0.50907	2.60453
4 2			
Direct			
	0.74709	0.40174	0.49419
	0.22655	0.09891	0.45310
	0.77345	0.90109	0.54690
	0.25291	0.59826	0.50581
	0.50000	0.11905	0.00000
	0.76190	0.61905	0.00000

NEB-13			
H4 P2			
1.00000			
	2.58122	0.00000	0.00000
	0.00000	3.46983	0.00890
	-1.29061	-0.46101	2.60163
4 2			
Direct			
	0.74484	0.40318	0.48969
	0.22641	0.09753	0.45281
	0.77359	0.90247	0.54719
	0.25516	0.59682	0.51031
	0.50000	0.10714	0.00000
	0.78571	0.60714	0.00000

NEB-14			
H4 P2			
1.00000			
	2.62336	0.00000	0.00000
	0.00000	3.41305	0.00964
	-1.31168	-0.41294	2.59873
4 2			
Direct			
	0.74259	0.40461	0.48518
	0.22626	0.09616	0.45252
	0.77374	0.90384	0.54748
	0.25741	0.59539	0.51482
	0.50000	0.09524	0.00000
	0.80952	0.59524	0.00000

NEB-15			
H4 P2			
1.00000			
	2.66550	0.00000	0.00000
	0.00000	3.35627	0.01038
	-1.33275	-0.36488	2.59583
4 2			
Direct			
	0.74034	0.40605	0.48068
	0.22612	0.09478	0.45224
	0.77388	0.90522	0.54776
	0.25966	0.59395	0.51932
	0.50000	0.08333	0.00000
	0.83333	0.58333	0.00000

NEB-16			
H4 P2			
1.00000			
	2.70763	0.00000	0.00000
	0.00000	3.29950	0.01113
	-1.35382	-0.31681	2.59293
4 2			
Direct			
	0.73809	0.40749	0.47618
	0.22597	0.09340	0.45195
	0.77403	0.90660	0.54805
	0.26191	0.59251	0.52382
	0.50000	0.07143	0.00000
	0.85714	0.57143	0.00000

NEB-17			
H4 P2			
1.00000			
	2.74977	0.00000	0.00000
	0.00000	3.24272	0.01187
	-1.37488	-0.26875	2.59002
4 2			
Direct			
	0.73584	0.40892	0.47167
	0.22583	0.09202	0.45166
	0.77417	0.90798	0.54834
	0.26416	0.59108	0.52833
	0.50000	0.05952	0.00000
	0.88095	0.55952	0.00000

NEB-18			
H4 P2			
1.00000			
	2.79191	0.00000	0.00000
	0.00000	3.18595	0.01261
	-1.39595	-0.22068	2.58712
4 2			
Direct			
	0.73359	0.41036	0.46717
	0.22568	0.09064	0.45137
	0.77432	0.90936	0.54863
	0.26641	0.58964	0.53283
	0.50000	0.04762	0.00000
	0.90476	0.54762	0.00000

NEB-19			
H4 P2			
1.00000			
	2.83404	0.00000	0.00000
	0.00000	3.12917	0.01335
	-1.41702	-0.17262	2.58422
4 2			
Direct			
	0.73133	0.41180	0.46267
	0.22554	0.08927	0.45108
	0.77446	0.91073	0.54892
	0.26867	0.58820	0.53733
	0.50000	0.03571	0.00000
	0.92857	0.53571	0.00000

NEB-20			
H4 P2			
1.00000			
	2.87618	0.00000	0.00000
	0.00000	3.07239	0.01409
	-1.43809	-0.12455	2.58132
4 2			
Direct			
	0.72908	0.41324	0.45816
	0.22540	0.08789	0.45079
	0.77460	0.91211	0.54921
	0.27092	0.58676	0.54184
	0.50000	0.02381	0.00000
	0.95238	0.52381	0.00000

NEB-21			
H4 P2			
1.00000			
	2.91832	0.00000	0.00000
	0.00000	3.01562	0.01484
	-1.45916	-0.07649	2.57842
4 2			
Direct			
	0.72683	0.41467	0.45366
	0.22525	0.08651	0.45050
	0.77475	0.91349	0.54950
	0.27317	0.58533	0.54634
	0.50000	0.01190	0.00000
	0.97619	0.51190	0.00000

NEB-22			
H4 P2			
1.00000			
	2.96046	0.00000	0.00000
	0.00000	2.95884	0.01558
	-1.48023	-0.02842	2.57552
4 2			
Direct			
	0.72458	0.41611	0.44916
	0.22511	0.08513	0.45021
	0.77489	0.91487	0.54979
	0.27542	0.58389	0.55084
	0.50000	0.00000	0.00000
	0.00000	0.50000	0.00000

Table S18: Stepwise VASP POSCARs for NEB images. NEB-13 is the transition state.

References

[S1] D. C. Lonie and E. Zurek, *Comput. Phys. Commun.*, **2011**, *182*, 372–387.

[S2] D. C. Lonie and E. Zurek, *Comput. Phys. Commun.*, **2011**, *182*, 2305–2306.

[S3] J. C. Jamieson, *Science*, **1963**, *139*, 1291–1292.

[S4] T. Kikegawa and H. Iwasaki, *Acta Cryst.*, **1983**, *B39*, 158–164.

[S5] Y. Akahama, M. Kobayashi and H. Kawamura, *Phys. Rev. B.*, **1999**, *59*, 8520.

[S6] C. J. Pickard and R. J. Needs, *Nat. Phys.*, **2007**, *3*, 473–476.